NACA RM No. L8K12

NACA

RESEARCH MEMORANDUM

LATERAL-CONTROL INVESTIGATION ON A 37° SWEPTBACK WING OF ASPECT RATIO 6 AT A REYNOLDS NUMBER OF 6,800,000

By

Robert R. Graham and William Koven

Langley Aeronautical Laboratory
Langley Field, Va.

NATIONAL ADVISORY COMMITTEE
FOR AERONAUTICS

WASHINGTON
January 27, 1949

NACA RM No. L8K12

NATIONAL ADVISORY COMMITTEE FOR AERONAUTICS

RESEARCH MEMORANDUM

LATERAL-CONTROL INVESTIGATION ON A 37° SWEPTBACK WING OF ASPECT RATIO 6 AT A REYNOLDS NUMBER OF 6,800,000

By Robert R. Graham and William Koven

SUMMARY

The low-speed lateral-control characteristics of a 37° sweptback semispan wing of aspect ratio 6 and NACA 64-series airfoil sections have been determined in the Langley 19-foot pressure tunnel. The investigation included the measurement of the hinge-moment characteristics of an aileron and the rolling-effectiveness characteristics of the aileron and two configurations of spoilers. The effects of several stall-control and high-lift devices on the characteristics of the aileron and spoiler were also investigated. The tests were made at a Reynolds number of 6,800,000.

The rate of change of rolling-moment coefficient with aileron deflection C_{l_δ} for a half-span, 20-percent-chord aileron on the plain wing decreased almost linearly from 0.00146 at 0° angle of attack to 0.00100 at 18° angle of attack. Beyond 18° the value of C_{l_δ} decreased rapidly as the wing stalled. The value of C_{l_δ} at 0° angle of attack was accurately predicted by simple theory.

All the stall-control devices tested were satisfactory in maintaining aileron effectiveness through the high angle-of-attack range to beyond maximum lift.

The rate of change of hinge-moment coefficient with deflection C_{h_δ} for the unbalanced aileron was reduced in some cases and increased in others by the addition of the various stall-control and high-lift devices; however, the effects of the devices on the size of internal balance required to reduce C_{h_δ} to zero were found to be small because of the corresponding effects on the balance-compartment pressures.

The stall-control devices brought about some improvement in spoiler effectiveness throughout the lift range and caused the spoilers to maintain their effectiveness to the highest angle of attack tested.

Shifting the spoiler location from the 65- to 75-percent-chord line of the unswept panel caused a slight improvement in spoiler effectiveness.

Changing the spoiler from a continuous one along the 65-percent-chord line of the unswept panel to a series of segments with their midpoints

on the same line but turned perpendicular to the air stream had practically no effect on the rolling effectiveness, but moving the segments inboard caused an increase in effectiveness.

Varying the span of the spoiler showed that the inboard portions of the spoiler were considerably more effective than the outboard portions in producing rolling moments.

At high lift coefficients on the wing with slat and double slotted flap, the half-span plain outboard spoiler with a 10-percent-chord projection produced about the same rolling moment as a total aileron deflection of 30°, but at low lift coefficients on the plain wing the spoiler produced only about one-third the rolling moment of the ailerons.

The yawing moments due to oppositely deflected ailerons were generally unfavorable and became more unfavorable as the angle of attack was increased. Those due to spoiler projection were favorable but became less favorable as the angle of attack was increased or as the spoiler was moved inboard. The stall-control and high-lift devices had a negligible effect on the yawing moments.

INTRODUCTION

The use of sweptback wings on high-speed airplanes introduces several stability and control problems in the low-speed range. Two of these problems are unstable pitching moments and loss of lateral control at the stall. Both of these problems result from the characteristic of sweptback wings to stall first at the tips.

Several devices have been found to delay the tip stall until an inboard stall has developed so that stable pitching moments were obtained at the stall. (See references 1 and 2.) These devices were leading-edge flap, leading-edge slat, and drooped leading edge on the outer portion of the wing.

In order to determine the effects of these devices on the lateral-control characteristics of a sweptback wing, an investigation was carried out on a 37° sweptback semispan wing of aspect ratio 6. The investigation included the determination of (a) the control and hinge-moment characteristics of a half-span 20-percent-chord aileron, (b) the control characteristics of two configurations of spoilers, and (c) the effects of high-lift and stall-control devices on the characteristics of the aileron and spoilers.

COEFFICIENTS AND SYMBOLS

The data are referred to the wind axes with the origin in the plane of symmetry at the quarter chord of the mean aerodynamic chord. The data have been reduced to standard NACA nondimensional coefficients which are defined as follows:

C_L lift coefficient $\left(\frac{L}{qS}\right)$

C_D drag coefficient $\left(\frac{D}{qS}\right)$

C_m pitching-moment coefficient $\left(\frac{M}{qS\bar{c}}\right)$

C_l rolling-moment coefficient $\left(\frac{L'}{qSb}\right)$

C_n yawing-moment coefficient $\left(\frac{N}{qSb}\right)$

C_{h_a} aileron hinge-moment coefficient $\left(\frac{H_a}{2M_a q}\right)$

P_R resultant pressure coefficient in aileron balance compartment $\left(\frac{\text{Pressure below seal - Pressure above seal}}{q}\right)$

E aileron-seal leakage factor $\left[1 - \frac{\text{Pressure difference across seal}}{\text{Pressure difference across vents}}\right]$

R Reynolds number $\left(\frac{\rho V\bar{c}}{\mu}\right)$

α angle of attack of root chord line, degrees

δ_a aileron deflection measured in plane perpendicular to hinge line (positive when deflected down), degrees

Λ angle of sweep of leading edge

L lift

D drag

M pitching moment about $0.25\bar{c}$

L'	rolling moment
N	yawing moment
H_a	aileron hinge moment
S	wing area
$\bar{c}$	mean aerodynamic chord $\left(\frac{2}{S}\int_0^{b/2} c^2 \, dy\right)$
c	local wing chord parallel to plane of symmetry
c'	local wing chord perpendicular to 0.27c line
A	aspect ratio $\left(\frac{b^2}{S}\right)$
y	lateral coordinate
b	wing span perpendicular to plane of symmetry
M_a	moment of area of aileron rearward of hinge line about hinge axis
b_a	aileron span measured along hinge line
b_s	spoiler span measured perpendicular to plane of symmetry
c_a	aileron chord rearward of hinge line measured perpendicular to 0.27c line
c_b	aileron nose-balance chord forward of hinge line measured perpendicular to 0.27c line
q	dynamic pressure $\left(\frac{\rho V^2}{2}\right)$
ρ	density of air
V	free-stream velocity
μ	coefficient of viscosity
C_{l_δ}	rate of change of rolling-moment coefficient with aileron deflection
C_{L_δ}	rate of change of lift coefficient with aileron deflection

C_{h_δ} rate of change of aileron hinge-moment coefficient with aileron deflection

P_{R_δ} rate of change of resultant-pressure coefficient with aileron deflection

C_{h_α} rate of change of aileron hinge-moment coefficient with angle of attack

P_{R_α} rate of change of resultant-pressure coefficient with angle of attack

All coefficients and dimension symbols refer to the model as a complete wing. The effects of the spoiler controls on lift, drag, and pitching-moment coefficients are presented as the effects of spoiler projection on one side of a complete wing.

MODEL

The model used in the investigation was a semispan wing mounted in the presence of a reflection plane as shown in figures 1 and 2. It was of steel construction and had an aspect ratio of 6, a taper ratio of 0.5, and 37° sweepback of the leading edge. The airfoil section perpendicular to the 27-percent-chord line (25-percent-chord line of wing when in the unswept condition) was an NACA 64_1-212 profile. The model was finished with lacquer and was maintained in an aerodynamically smooth condition throughout the tests. The general plan form and some of the more pertinent dimensions of the model are shown in figure 3.

Details of the lateral-control devices are shown in figure 4. The aileron was of the constant-percentage-chord type (0.20c' or 0.183c) and had the same contour as the corresponding portion of the airfoil section. It was arranged to simulate a sealed internally balanced type of aileron with zero balance. The seal was simulated by a steel plate beveled to a knife edge with the edge as close as possible to the nose of the aileron at the hinge line. Although this method did not completely seal the aileron, the resulting gap was only a small fraction of the balance-compartment vents at the upper and lower surfaces of the wing. The balance compartment was provided with orifices for measuring pressures above and below the seal. The aileron was attached to the wing by strain gages which indicated electrically the aileron hinge moments.

Two configurations of spoiler lateral controls were investigated. One extended along a constant-percentage-chord line and the other consisted of a series of spoilers, each 10 percent of the wing semispan in length and placed perpendicular to the plane of symmetry. The first is referred to herein as the plain spoiler and the second as the step spoiler.

Both configurations simulated retractable circular-arc spoilers. Various projections of the plain spoiler were tested at the $0.65c'$ and $0.75c'$ positions, but only one projection of the step spoiler was tested with the midpoint of each step at $0.65c'$. The projection of the plain spoiler was a constant percent chord along the span, but the step spoiler projection varied in steps along the span. The height at the center of each step was a constant percent chord but the individual steps were a constant height along the span of each step.

The aileron and plain spoiler extended from $0.500\frac{b}{2}$ to $0.975\frac{b}{2}$. The step spoiler extended from $0.275\frac{b}{2}$ to $0.975\frac{b}{2}$, but the span and spanwise location could be varied by varying the number and location of the steps.

Details of the leading-edge stall-control devices and of the trailing-edge high-lift devices are shown in figure 5. The stall-control devices consisted of a leading-edge flap, leading-edge slat, and drooped leading edge and extended from $0.45\frac{b}{2}$ to $0.95\frac{b}{2}$. The drooped leading edge was tested only in combination with an upper-surface fence because a previous investigation (reference 1) showed that it was not a satisfactory stall-control device without the fence. The trailing-edge high-lift devices were half-span split and double slotted flaps.

TESTS

The tests were made in the Langley 19-foot pressure tunnel with the air compressed to about $2\frac{1}{3}$ atmospheres. The Reynolds and Mach numbers for the tests were 6,800,000 and 0.13, respectively.

Rolling-effectiveness tests for the various lateral-control devices were made by taking six-component force and moment measurements through a range of angle of attack from 0° to beyond the stall with the aileron set at various angles or with the spoilers set at various heights, spans, and spanwise locations. Hinge moments and balance-compartment pressures were also measured in the aileron tests. The tests were made on the basic wing, on the wing with the various stall-control devices, and on the wing with the slat in combination with split or double slotted flaps.

CORRECTIONS TO DATA

Jet-boundary corrections, obtained by combining the methods of references 3 and 4 were made to the angle of attack and to the drag, pitching-moment, yawing-moment, and rolling-moment coefficients. The corrections were applied as follows:

$$\alpha = \alpha_{geometric} + 1.12\, C_L$$

$$C_D = C_{D_{gross}} + 0.0164\, C_L^2$$

$$C_m = C_{m_{gross}} + 0.0101\, C_L$$

$$C_l = K_l\left(C_{l_{gross}} - C_{l_{tare}}\right)$$

$$C_n = C_{n_{gross}} - C_{n_{tare}} - K_n\, C_L\, C_l$$

where the subscript "gross" refers to the uncorrected coefficients, the subscript "tare" refers to the uncorrected coefficients obtained with aileron or spoiler neutral, and K_l and K_n are the rolling-moment and yawing-moment jet-boundary-correction constants. Values for K_l are presented in figure 6 for various spans and spanwise locations of the lateral control. The values of K_n would show similar variations; but since yawing-moment data are not presented for all configurations tested, only those values applicable to the data presented are given: namely, 0.0481 for a half-span lateral control with the outboard end at $0.975\frac{b}{2}$ and 0.0578 for a half-span lateral control with the outboard end at $0.775\frac{b}{2}$. No jet-boundary corrections have been applied to the aileron hinge-moment data.

A calibration of the aileron seal indicated a leakage factor E of 0.14. The balance-compartment pressures have been corrected for this leakage so that they represent pressures with a complete seal. The effects of the leakage on the rolling-moment and hinge-moment coefficients, however, are believed to be small and have been neglected.

The tare and interference effects of the model supports were not determined but are believed to have only a small effect on the characteristics of the wing.

RESULTS AND DISCUSSION

The results of the aileron investigation are presented in figure 7 for the basic wing and in figures 8 to 12 for the wing with the various stall-control and high-lift devices. Summary figures showing the effects of the various devices on the aileron hinge-moment and rolling-effectiveness parameters are shown in figures 13 to 16. The results of the spoiler investigation are presented in figures 17 to 20 for the basic wing and figures 21 to 27 for the wing with the various stall-control and high-lift devices. A comparison of the aileron and spoilers is presented in figure 28.

Aileron Characteristics

Aileron characteristics on basic wing.- The data for the aileron tests on the plain wing are presented in figure 7. The control-effectiveness parameter C_{l_δ} was obtained from cross plots of the data of figure 7 and is presented as a function of angle of attack in figure 13.

The loss in aileron effectiveness that is usually found on sweptback wings at high angles of attack is clearly shown in figure 13. The reduction in C_{l_δ} at angles of attack below the stall is probably caused by the thickened boundary layer due to the cross flow along the trailing edge near the wing tips and the large reduction at the stall is attributed to tip stalling.

The value of C_{l_δ} for low angles of attack has been calculated by the method given in reference 5. The computed C_{l_δ} when reduced by $\cos^2\Lambda$ to account for sweep (reference 6) and corrected for section-lift-curve slope (0.109 for 64-series compared to 0.099 used to obtain required factors in reference 5) was 0.00145. The C_{l_δ} obtained experimentally at $\alpha = 0^\circ$, 0.00146, (fig. 13) was in excellent agreement with the simple-theory calculations.

The effectiveness of the aileron as a lift flap C_{L_δ} has been calculated from two-dimensional data by a method for unswept wings outlined in reference 7. The method was modified to account for sweep as was done in reference 1. The calculated value of C_{L_δ} was 0.0116 as compared with the experimental value of 0.0107 (data not presented). The agreement is not as good as was obtained for C_{l_δ} but is considered satisfactory. Values of C_{l_δ} and C_{L_δ} calculated by the method of reference 8 and corrected for section-lift-curve slope were 0.00143 and 0.0108, respectively, and show very good agreement with the experimental values.

The yawing-moment coefficients due to aileron deflection show about the same trends as would be expected on an unswept wing. They show that oppositely deflected ailerons on a complete wing would produce an adverse yawing moment which is small in the low angle-of-attack range but which increases as the angle of attack is increased.

The effects of the trailing-edge cross flow and tip stalling also appeared in the hinge-moment and balance-pressure coefficients. (See figures 7 and 15.) As the angle of attack was increased above 10°, the parameter C_{h_α} increased negatively until at the stall it had a very large negative value resulting in a strong up-floating tendency of the aileron. The parameter C_{h_δ}, on the other hand, had a decreasing negative value as α was increased.

Effects of stall-control and high-lift devices on aileron characteristics.- The characteristics of the aileron on the wing with various stall-control devices are shown in figures 8 to 12. The effects of the stall-control and high-lift devices on the various aileron control-effectiveness, hinge-moment, and balance-compartment-pressure parameters are shown in figures 13 to 16.

Figure 13 shows that the stall-control devices caused a decrease in C_{l_δ} at low angles of attack. At high angles of attack and especially at angles beyond that at which the plain wing stalled, C_{l_δ} was increased by the stall-control devices. The 30° drooped leading edge with the upper-surface fence caused the largest increase in C_{l_δ} at the high angles of attack. Split flaps in combination with the slat generally caused a reduction in C_{l_δ} from that for the wing alone throughout the angle-of-attack range.. Double slotted flaps in combination with the slat effected an increase in C_{l_δ} at all angles of attack.

The effects of the various stall-control devices on the rolling-moment coefficient for a total aileron deflection of 30° are shown in figure 14. All the stall-control devices reduced C_l at $\alpha = 0°$, had a negligible effect at moderate angles of attack, increased C_l at high angles of attack, and prevented the large loss in C_l that occurred at the stall of the basic wing. The leading-edge flap caused the largest reduction in C_l at $\alpha = 0°$ and all the devices produced about the same change at high angles of attack. The split flap in combination with the slat caused a slight reduction in C_l from that with the slat alone in the high angle-of-attack range. The C_l with double slotted flap in combination with the slat was larger than that for any other configuration in the low and moderate angle-of-attack range.

The stall-control and high-lift devices had a negligible effect on the yawing-moment coefficients due to oppositely deflected ailerons. (See figs. 7 to 12.)

The effects of the stall-control devices on the aileron hinge-moment parameters are shown in figures 15 and 16. In general the negative value of C_{h_α} was increased at low angles of attack and decreased at high angles of attack by the addition of the stall-control devices. The leading-edge flap caused the largest increase in C_{h_α} at the low angles of attack and caused a slight increase in C_{h_α} in the high angle-of-attack range in contrast to the decreases brought about by the slat and drooped leading edge at those angles. The addition of the split or double slotted flaps reduced the effects of the slat on C_{h_α}.

The negative value of C_{h_δ} was decreased by the stall-control devices in the low angle-of-attack range and increased at the higher angles of

attack. The addition of half-span split flaps caused a slight reduction in the negative value of C_{h_δ} obtained with the slat alone in place, but the addition of half-span double slotted flaps caused a considerable increase in C_{h_δ}.

These changes in C_{h_δ} are reduced considerably, however, when the effects of rolling are taken into account and when a sealed internal balance is added to the aileron. The effects of rolling can be taken into account by the following equation:

$$C_{h_\delta}' = C_{h_\delta} + \frac{2(\Delta\alpha)_p}{\Delta\delta_a} C_{h_\alpha}$$

where

C_{h_δ}' rate of change of aileron hinge moment with deflection when the wing is in a steady roll

$\frac{2(\Delta\alpha)_p}{\Delta\delta_a}$ ratio of effective change in angle of attack to aileron deflection in a steady roll (The value of $\frac{2(\Delta\alpha)_p}{\Delta\delta_a}$ was found to be $-.168C_{l_\delta}$ from data given in references 9 and 10.)

The effects of the sealed internal balance can be taken into account by the following equations:

$$C_{h_{\alpha(bal)}} = C_{h_\alpha} + \tfrac{1}{2}\rho R_\alpha \left(\frac{c_b}{c_a}\right)^2$$

and

$$C_{h_{\delta(bal)}} = C_{h_\delta} + \tfrac{1}{2}\rho R_\delta \left(\frac{c_b}{c_a}\right)^2$$

where the subscript (bal) refers to the aileron with an internal nose balance and $\left(\frac{c_b}{c_a}\right)$ is the ratio of the nose-balance chord to the aileron chord. Values for C_{h_δ}' have been computed for several ratios of balance chord to aileron chord and for several angles of attack and are presented in figure 16.

It can be seen from figure 16 that although C_{h_δ}' for the unbalanced aileron is changed considerably by the stall-control devices, the balance chord required to reduce C_{h_δ}' to zero is affected to only a small degree by the devices. The value of C_{h_δ}' for the unbalanced aileron varies

from 0.0046 to 0.0089 for the various angles of attack and configurations investigated, but the balance chord required to reduce C_{h_δ}' to zero varies only between 65 and 75 percent of the aileron chord and bears no relation to the value for the unbalanced aileron. For instance, at an angle of attack of 2° the value of C_{h_δ}' was increased from -0.0071 to -0.0089 by extending the slat and deflecting the double slotted flap, but the balance chord required to reduce C_{h_δ}' to zero was reduced from about 75 to 70 percent of the aileron chord.

Spoiler Characteristics

Spoiler characteristics on basic wing.- The characteristics of spoilers as lateral-control devices on the basic wing are shown in figures 17 to 20. The rolling effectiveness of the spoiler increases with angle of attack up to about 12°. Above that angle the effectiveness drops off slightly until just below the stall where an apparent increase in effectiveness occurs. At the stall the effectiveness drops to zero. The loss in effectiveness at angles of attack between 12° and 16° is probably caused by the thickened boundary layer due to cross flow over the outboard sections. The apparent increase in effectiveness just below the stall is probably caused by premature separation over the outer portion of the wing due to the presence of the spoiler. The separation was not severe enough to cause an appreciable loss in lift, but its effects show up as a change in drag and pitching moment as well as rolling moment and yawing moment. At the angle of attack of maximum lift the 0.01c' spoiler caused as much separation as the 0.10c' spoiler so that the three spoiler heights tested caused the same rolling moment. The lift, drag, and pitching-moment coefficients at the angle of attack for maximum lift were also the same regardless of spoiler projection. The complete loss in effectiveness beyond maximum lift is due to the tip stall. Comparison of figures 17 and 18 shows that the spoiler effectiveness is increased slightly when the spoiler is moved from the 0.65c' location to the 0.75c' location. This effect of chordwise location is in agreement with that shown in reference 11.

The yawing-moment coefficients due to spoiler projection showed about the same trends as would be expected from unswept wing data (reference 12). They were in a favorable direction but became less favorable as the angle of attack was increased. Moving the spoiler toward the trailing edge from 0.65c' to 0.75c' reduced the yawing-moment coefficients.

The characteristics of the step spoiler are shown in figure 19. Comparison of figure 19 with figure 17 shows that a step spoiler of the same span, spanwise location, and projection as the plain spoiler produced about the same rolling moment as the plain spoiler except at angles of attack just below the stall where the step spoiler showed a slight improvement over the plain spoiler. These data are in disagreement with data of reference 11 where a step spoiler on a wing of lower aspect ratio

and slightly greater sweep showed greater rolling effectiveness than a comparable plain spoiler. No explanation has been found for the disagreement but it may be due to the difference in the geometric characteristics of the wings. The step spoilers caused a slightly smaller yawing moment than the plain spoiler.

Moving the spoiler inboard but maintaining the same span caused an appreciable increase in its effectiveness, which is in general agreement with the results of reference 11. The inboard movement of the spoiler also caused a reduction in yawing-moment coefficient.

The effects on the rolling effectiveness of varying the span and the spanwise location of the step spoiler are shown in figure 20. It can be seen that the addition of the outboard portions of the step spoiler adds little to the effectiveness of the inboard spoiler. Inboard additions to the outboard spoiler, on the other hand, produced considerable increases in effectiveness.

It is believed that the plain spoiler would exhibit similar characteristics if its span and spanwise location were varied. It is also probable that changes in the geometry of the aileron would produce similar changes in effectiveness.

Effects of stall-control and high-lift devices on spoiler characteristics.- The effects of the various stall-control devices on the spoiler characteristics are shown in figures 21 to 27. The devices caused a slight improvement in the rolling effectiveness of the spoilers in the low and moderate angle-of-attack range. In the high angle-of-attack range the rolling effectiveness was considerably improved. The improvement at moderate to high angles of attack was probably caused by the stall-control devices reducing the cross flow. (See reference 1.) As the angle of attack was increased further, the improvement was effected by preventing stalling from occurring over the portion of the wing affected by the spoiler. The slat and the drooped leading edge with fence appeared to give the most improvement in effectiveness, but all three of the stall-control devices eliminated the complete loss in effectiveness at the stall that was experienced on the basic wing. Deflecting either the split or double slotted flaps in combination with the slat produced a considerable increase in rolling effectiveness for large spoiler projections.

The stall-control devices generally caused a slight increase in the spoiler yawing-moment coefficients at low angles of attack but caused no change at moderate angles of attack. Deflecting the split or double slotted flaps in conjunction with the slat caused a considerable increase in the spoiler yawing moments through the angle-of-attack range.

The effects of changing the span of the step spoiler in the presence of the leading-edge flap are shown in figure 25. It can be seen that in the low and moderate angle-of-attack ranges, changing the span of the

spoiler had about the same effect as on the basic wing. At the high angles of attack, however, the inboard spoiler loses effectiveness because of the inboard stall and the short-span spoiler, therefore, has more effectiveness near the tip than on the inboard portion of the wing.

Comparison of Spoiler and Aileron

A comparison of the rolling effectivenss of the plain spoiler and the aileron is shown in figure 28. It shows that near zero lift the rolling-moment coefficient produced by the spoiler was about the same as that produced by a total aileron deflection of only 9°. At a lift coefficient of 1.6, however, (slat and double slotted flap extended) the spoiler produced about the same rolling moment as a total aileron deflection of 30°. The 0.10c' projection of the spoiler was chosen as the maximum that could be obtained with a retractable-arc-type spoiler. The maximum deflection that could be obtained with a sealed internally balanced aileron on a wing similar to the model tested would be about ±15°. It can be seen, therefore, that at high lift coefficients the spoiler has about the same effectiveness as the aileron. At low lift coefficients the spoiler appears to be considerably less effective than the aileron, but spoilers have been shown to produce smaller wing twisting moments than ailerons (reference 13) and under high-speed-flight conditions where wing twist is an important factor the spoiler might compare more favorably. Also, unpublished data have shown that compressibility effects increase the effectiveness of spoilers and reduce the effectiveness of ailerons. The spoiler span could be increased without limiting the flap span and could thus improve the lateral control with a possible simultaneous increase in maximum lift. One way that lateral control could be increased for the aileron without changing the flap span would be to increase the deflection. The data (figs. 7 to 12) show that the aileron maintains most of its effectiveness to deflections of ±25°, but the large deflections would require a balance other than the conventional internal nose balance because of space limitations in the balance compartment.

In order to evaluate the rolling-moment coefficients in terms of flying qualities, values of the wing-tip helix angle in roll $pb/2V$ were computed from the equation:

$$\frac{pb}{2V} = \frac{C_l}{C_{l_p}}$$

A value for C_{l_p} (wing damping coefficient in roll) was obtained for an unswept wing of the same aspect ratio and taper ratio from data presented in reference 14 and was corrected for sweep to give a value of 0.366 by the following equation (reference 10):

$$C_{l_p} = \frac{(A + 4)\cos\Lambda}{A + 4\cos\Lambda} \left(C_{l_p}\right)_{\Lambda=0}$$

The value of $pb/2V$ obtained in this manner for a 0.10c' projection of the half-span spoiler varied from 0.035 at zero lift with flaps neutral to 0.102 near the stall with slat and double slotted flap deflected. The value of $pb/2V$ for a total aileron deflection of 30° was about 0.10 through the same range of test conditions.

These values of $pb/2V$ have not been corrected for compressibility and yawing effects. Reference 14 recommends reducing the values by 20 percent through the speed range as an empirical correction for both effects. The recommendation was based on a comparison of flight-test values with calculated values for the same airplanes. The flight tests, however, were made on airplanes that were conventional at the time of publication of reference 14, that is, without sweep and with aileron controls. Because of the large effective dihedral of swept wings, yawing would produce larger rolling moments than on an unswept wing. At low speeds, therefore, the reduction in $pb/2V$ due to yawing would be expected to be greater than the proposed 20 percent on a sweptback wing with conventional ailerons. In fact, in a fixed-rudder roll, the adverse yaw due to aileron deflection coupled with the adverse yaw due to rolling might produce a large enough angle of yaw to give a rolling moment that would completely counteract the rolling moment due to aileron deflection. The spoiler, on the other hand, causes favorable yawing moments and might produce larger values of $pb/2V$ than were calculated.

At high speeds, compressibility has an adverse effect on the rolling effectiveness of the aileron and a favorable effect on that of the spoiler. Also, the wing twisting moments are larger for the aileron than for the spoiler. In high-speed flight, therefore, the values of $pb/2V$ for the spoiler might be greater than those calculated and those for the aileron might be considerably less than 80 percent of the calculated values. It can be seen that any general comparison of rolling effectiveness of spoilers and ailerons from low-speed wind-tunnel tests is limited. In the high-lift range, a half-span spoiler projected 0.10c' would probably produce greater values of $pb/2V$ than half-span 0.20c' ailerons deflected ±15°. In the low-lift range, any comparison is inadequate unless compressibility and wing-twist effects are considered.

CONCLUSIONS

The results of the wind-tunnel investigation of lateral-control devices on a 37° sweptback wing of aspect ratio 6 indicate the following conclusions:

1. The rate of change of rolling-moment coefficient with aileron deflection C_{l_δ} for a half-span, 20-percent-chord aileron on the plain wing decreased almost linearly from 0.00146 at 0° angle of attack to 0.00100 at 18° angle of attack. Beyond 18° the value of C_{l_δ} decreased rapidly as the wing stalled. The value of C_{l_δ} at 0° angle of attack was accurately predicted by simple theory.

2. All of the stall-control devices tested were satisfactory in maintaining aileron effectiveness through the high angle-of-attack range to beyond maximum lift.

3. The rate of change of hinge-moment coefficient with deflection C_{h_δ} for the unbalanced aileron was reduced in some cases and increased in others by the addition of the various stall-control and high-lift devices; however, the effects of the devices on the size of internal balance required to reduce C_{h_δ} to zero were found to be small because of the corresponding effects on the balance-compartment pressures.

4. The stall-control devices brought about some improvement in spoiler effectiveness throughout the lift range and caused the spoilers to maintain their effectiveness to the highest angle of attack tested.

5. Shifting the spoiler location from the 65- to 75-percent-chord line of the unswept panel caused a slight improvement in spoiler effectiveness.

6. Changing the spoiler from a continuous one along the 65-percent-chord line of the unswept panel to a series of segments with their midpoints on the same line but turned perpendicular to the air stream had practically no effect on the rolling effectiveness, but moving the segments inboard caused an increase in effectiveness.

7. Varying the span of the spoiler showed that the inboard portions of the spoiler were considerably more effective than the outboard portions in producing rolling moments.

8. At high lift coefficients on the wing with slat and double slotted flap, the half-span plain outboard spoiler with a 10-percent-chord projection produced about the same rolling moment as a total aileron deflection of 30°, but at low lift coefficients on the plain wing the spoiler produced only about one-third the rolling moment of the ailerons.

9. The yawing moments due to oppositely deflected ailerons were generally unfavorable and became more unfavorable as the angle of attack was increased. Those due to spoiler projection were favorable but became less favorable as the angle of attack was increased or as the spoiler was moved inboard. The stall-control devices had a negligible effect on the yawing moments.

Langley Aeronautical Laboratory
National Advisory Committee for Aeronautics
Langley Field, Va.

REFERENCES

1. Koven, William, and Graham, Robert R.: Wind-Tunnel Investigation of the High-Lift and Stall-Control Devices on a 37° Sweptback Wing of Aspect Ratio 6 at High Reynolds Numbers. NACA RM No. L8D29, 1948.

2. Graham, Robert R., and Conner, D. William: Investigation of High-Lift and Stall-Control Devices on an NACA 64-Series 42° Sweptback Wing with and without Fuselage. NACA RM No. L7G09, 1947.

3. Sivells, James C., and Deters, Owen J.: Jet-Boundary and Plan-Form Corrections for Partial-Span Models with Reflection Plane, End Plate, or No End Plate in a Closed Circular Wind Tunnel. NACA Rep. No. 843, 1946.

4. Eisenstadt, Bertram J.: Boundary-Induced Upwash for Yawed and Swept-Back Wings in Closed Circular Wind Tunnels. NACA TN No. 1265, 1947.

5. Pearson, Henry A., and Jones, Robert T.: Theoretical Stability and Control Characteristics of Wings with Various Amounts of Taper and Twist. NACA Rep. No. 635, 1938.

6. Letko, William, and Goodman, Alex: Preliminary Wind-Tunnel Investigation at Low Speed of Stability and Control Characteristics of Swept-Back Wings. NACA TN No. 1046, 1946.

7. Pearson, Henry A., and Anderson, Raymond F.: Calculation of the Aerodynamic Characteristics of Tapered Wings with Partial-Span Flaps. NACA Rep. No. 665, 1939.

8. Lowry, John G., and Schneiter, Leslie E.: Estimation of Effectiveness of Flap-Type Controls on Sweptback Wings. NACA TN No. 1674, 1948.

9. Langley Research Department (Compiled by Thomas A. Toll): Summary of Lateral-Control Research. NACA TN No. 1245, 1947.

10. Toll, Thomas A., and Queijo, M. J.: Approximate Relations and Charts for Low-Speed Stability Derivatives of Swept Wings. NACA TN No. 1581, 1948.

11. Schneiter, Leslie E., and Watson, James M.: Low-Speed Wind-Tunnel Investigation of Various Plain-Spoiler Configurations for Lateral Control on a 42° Sweptback Wing. NACA TN No. 1646, 1948.

12. Fischel, Jack, and Tamburello, Vito: Investigation of Effect of Span, Spanwise Location, and Chordwise Location of Spoilers on Lateral Control Characteristics of a Tapered Wing. NACA TN No. 1294, 1947.

13. Fitzpatrick, James E., and Furlong, G. Chester: Effect of Spoiler-Type Lateral-Control Devices on the Twisting Moments of a Wing of NACA 230-Series Airfoil Sections. NACA TN No. 1298, 1947.

14. Swanson, Robert S., and Priddy, E. LaVerne: Lifting-Surface-Theory Values of the Damping in Roll and of the Parameter Used in Estimating Aileron Stick Forces. NACA ARR No. L5F23, 1945.

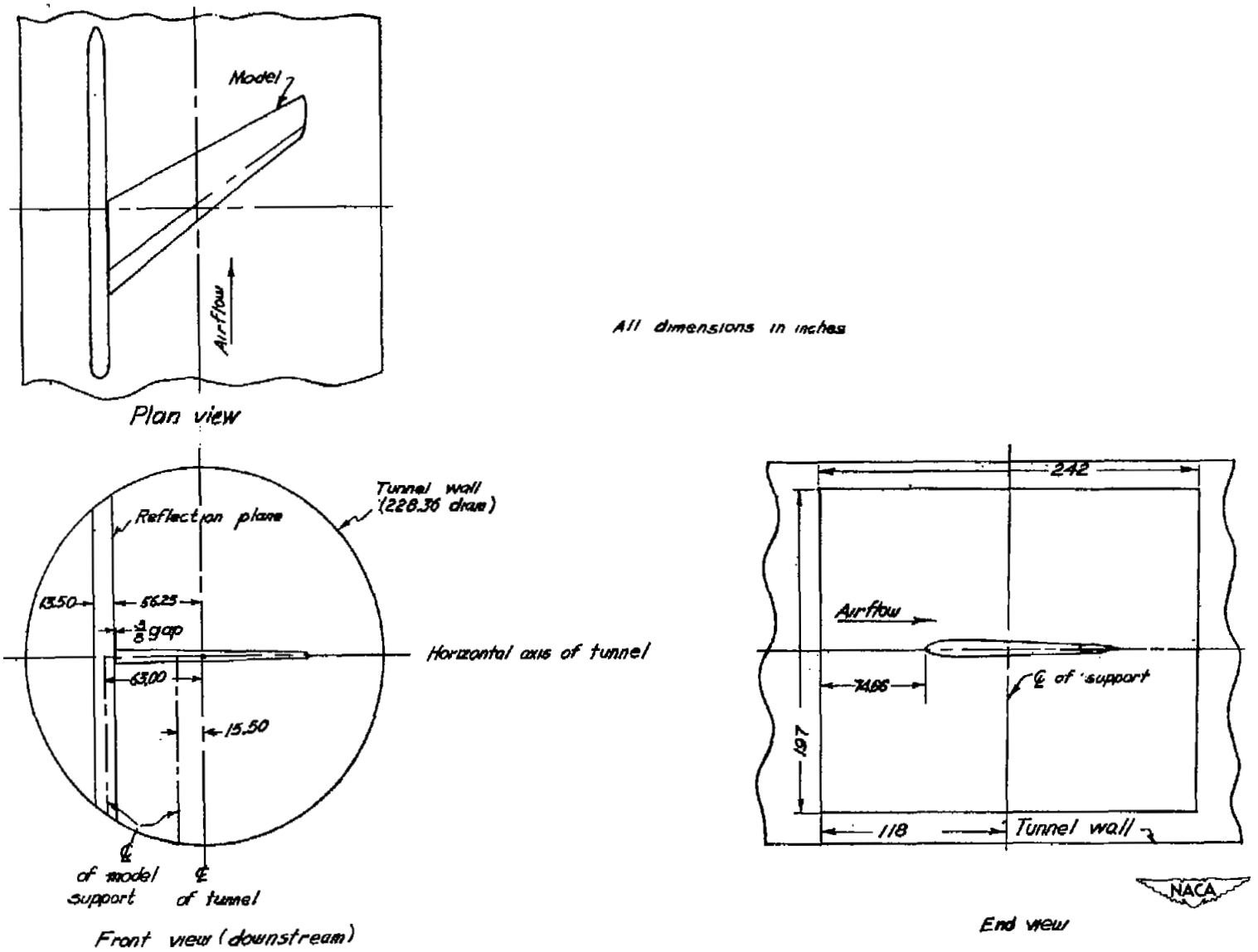

Figure 1.- Details of setup of 37° sweptback semispan wing and reflection plane in Langley 19-foot pressure tunnel.

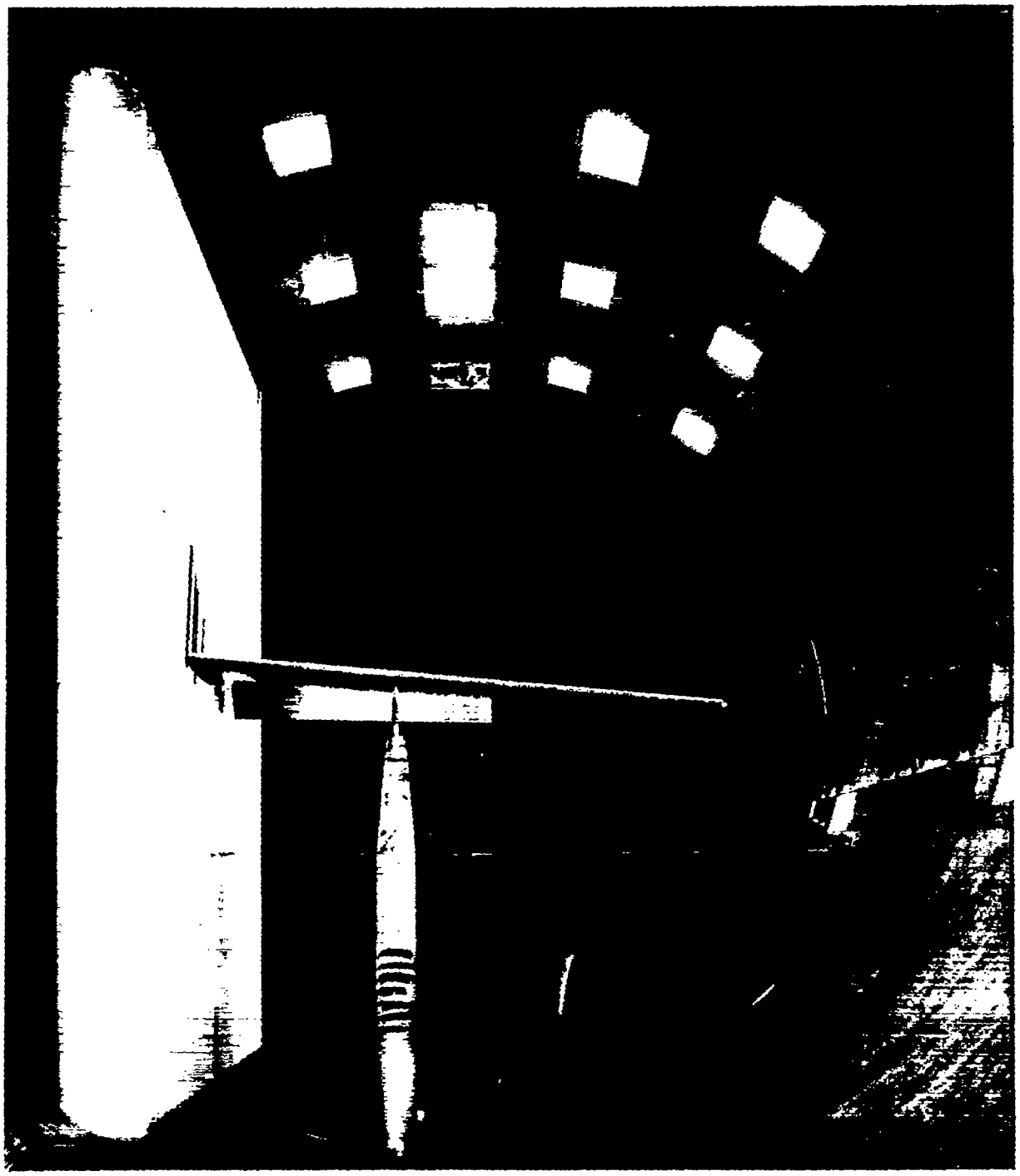

Figure 2.- Model and reflection plane mounted in tunnel.

NACA
L-54008.1

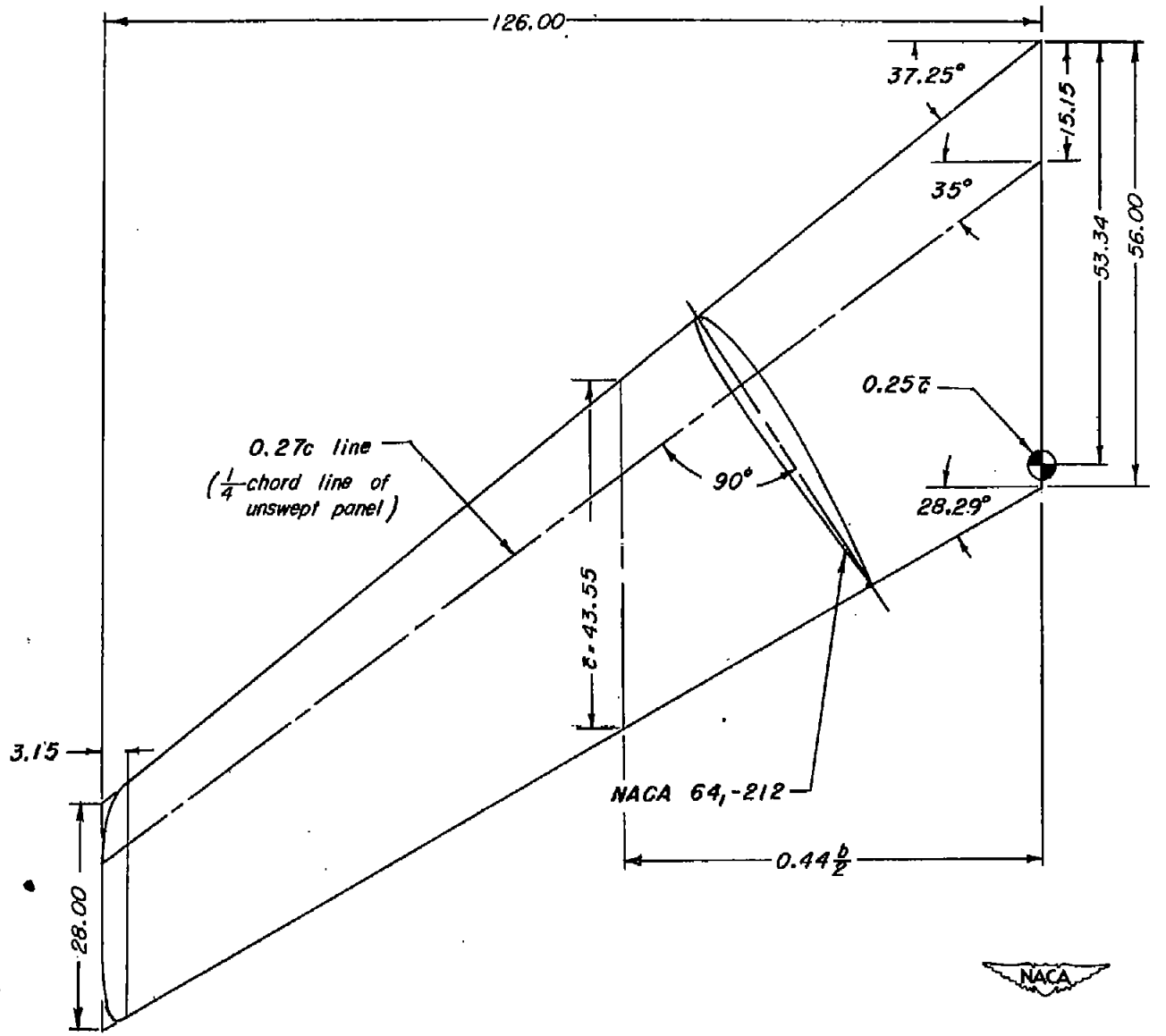

Figure 3.— General dimensions of model. Area (complete wing) = 73.2958 sq ft; aspect ratio = 6; taper ratio = 0.5. All dimensions in inches.

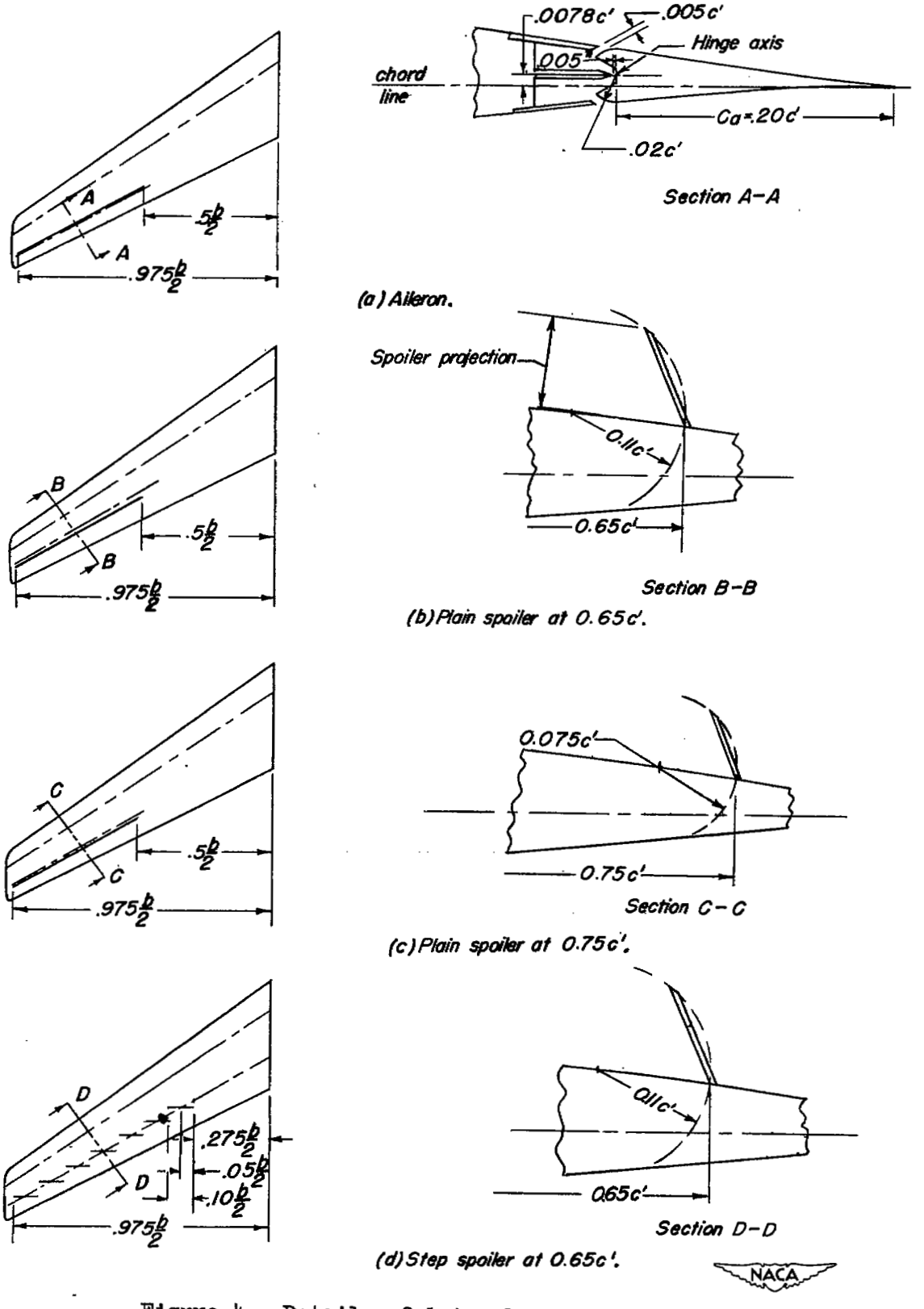

Figure 4.- Details of lateral-control devices.

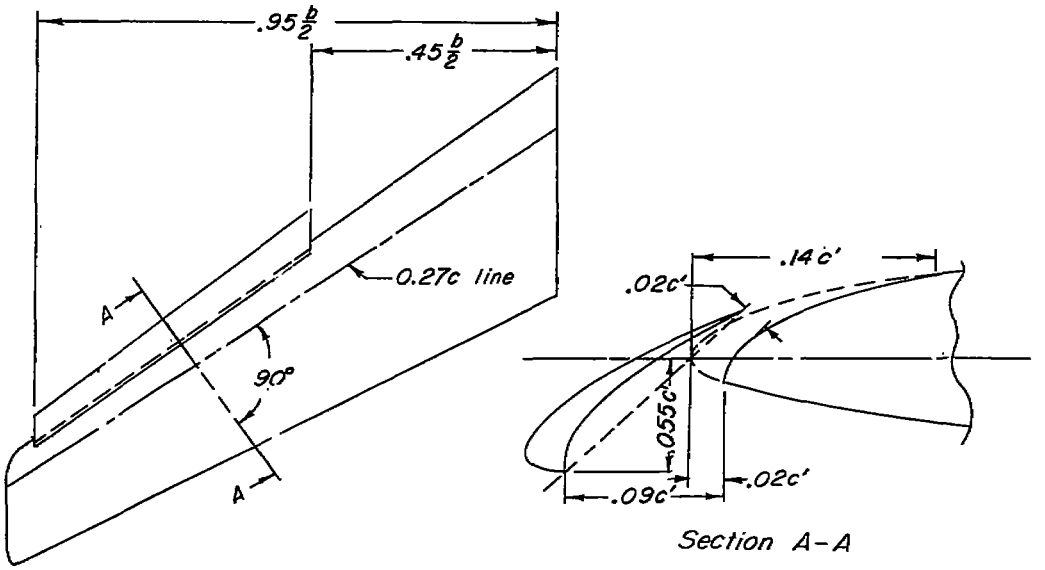

(a) Leading-edge slat.

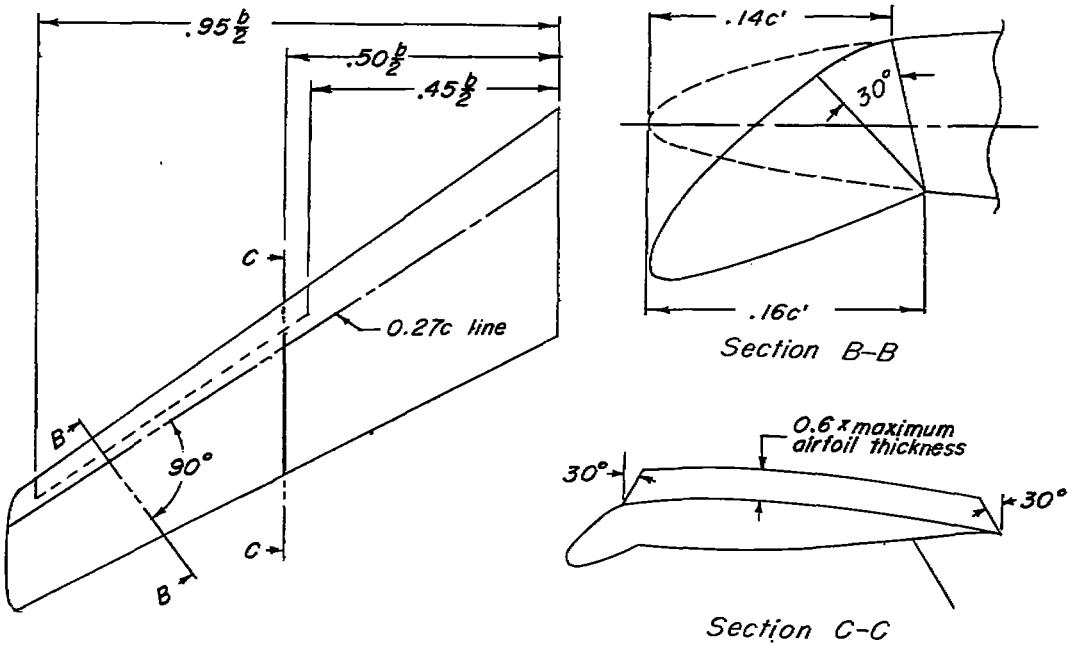

(b) Leading-edge droop with fence.

Figure 5.- Details of stall-control devices and trailing-edge flaps.

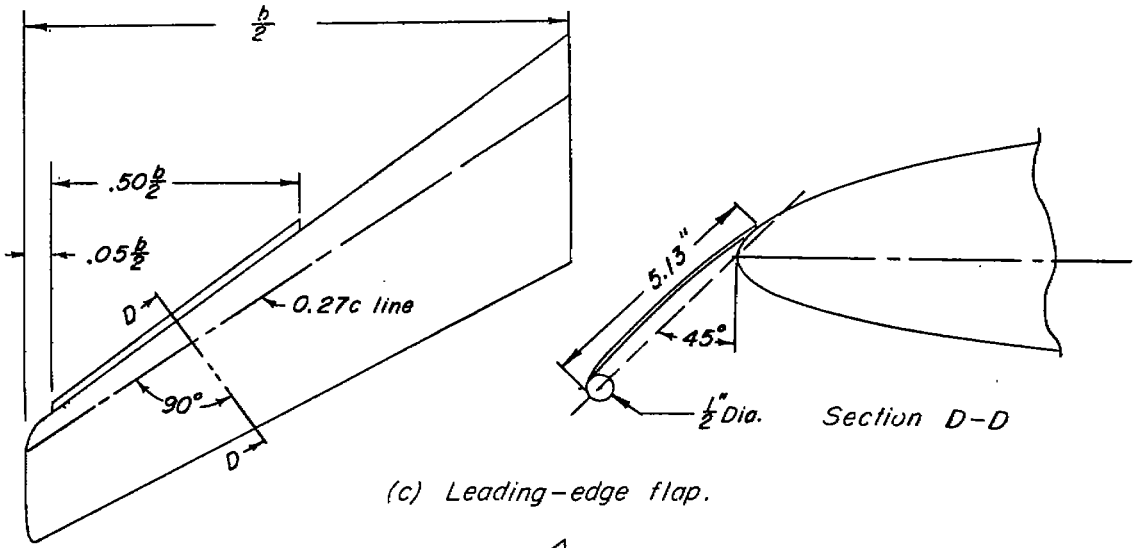

(c) Leading-edge flap.

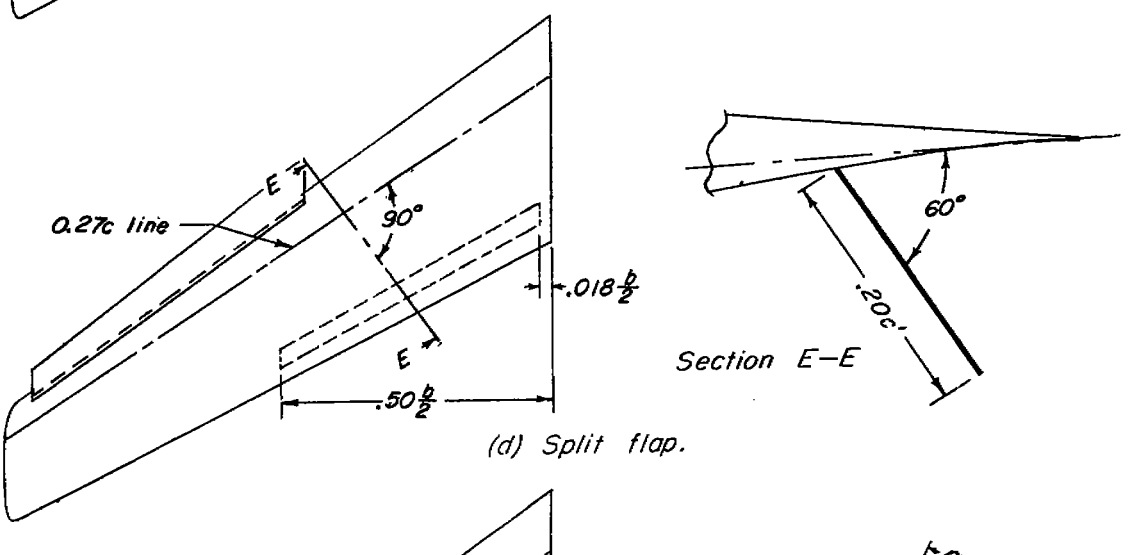

(d) Split flap.

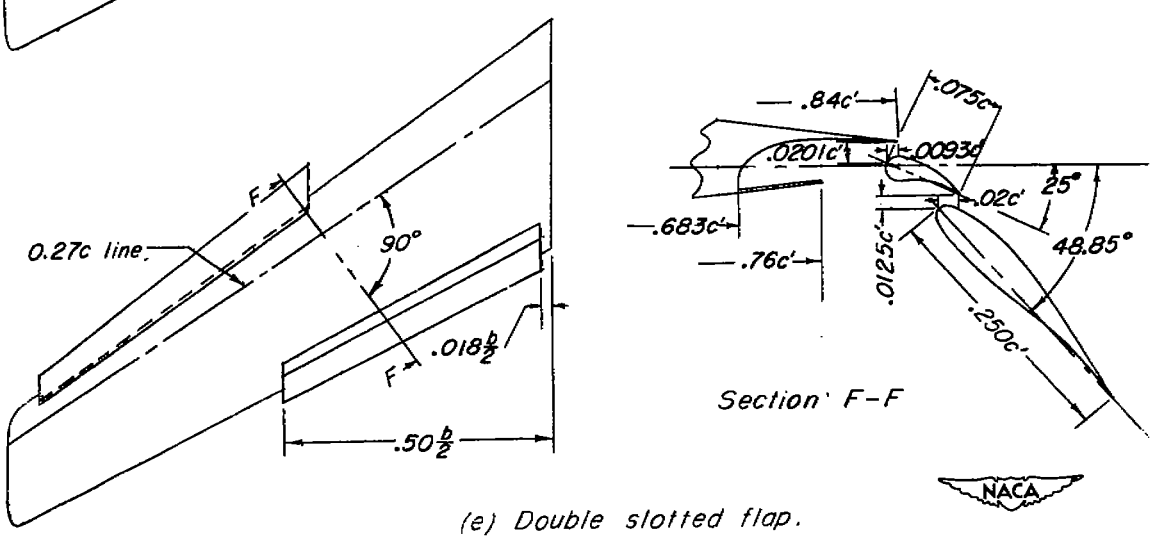

(e) Double slotted flap.

Figure 5.- Concluded.

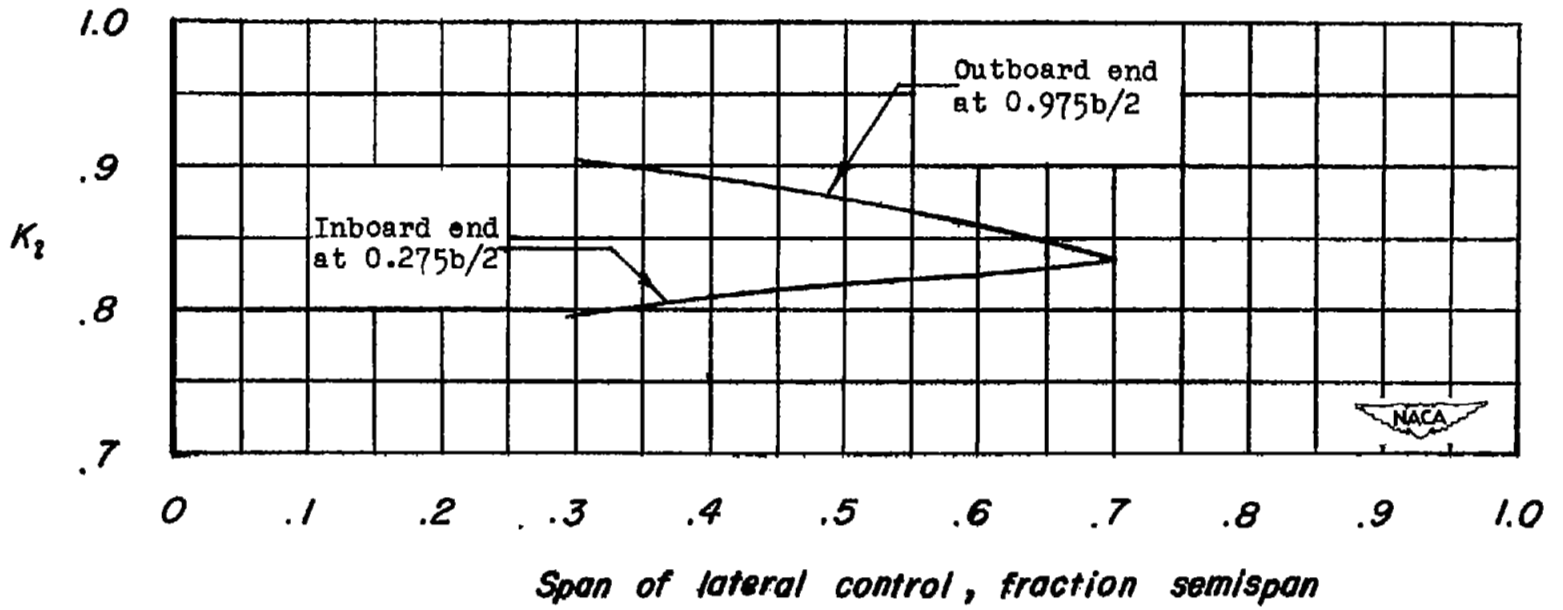

Figure 6.- Variation of jet-boundary rolling-moment correction factor with span of lateral control for two spanwise locations of control.

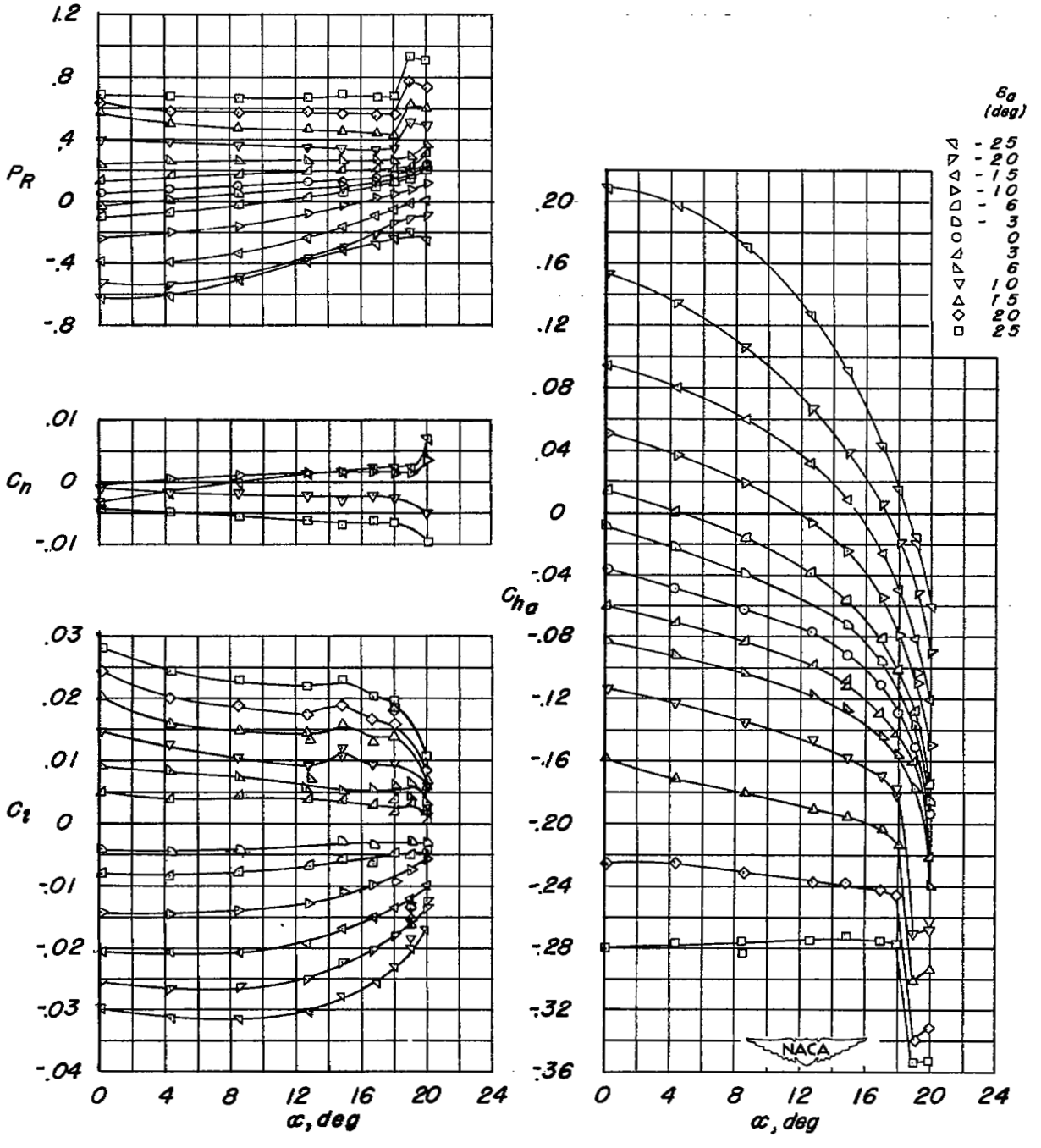

Figure 7.- Lateral control of a 37° sweptback wing and aileron. $R = 6.8 \times 10^6$.

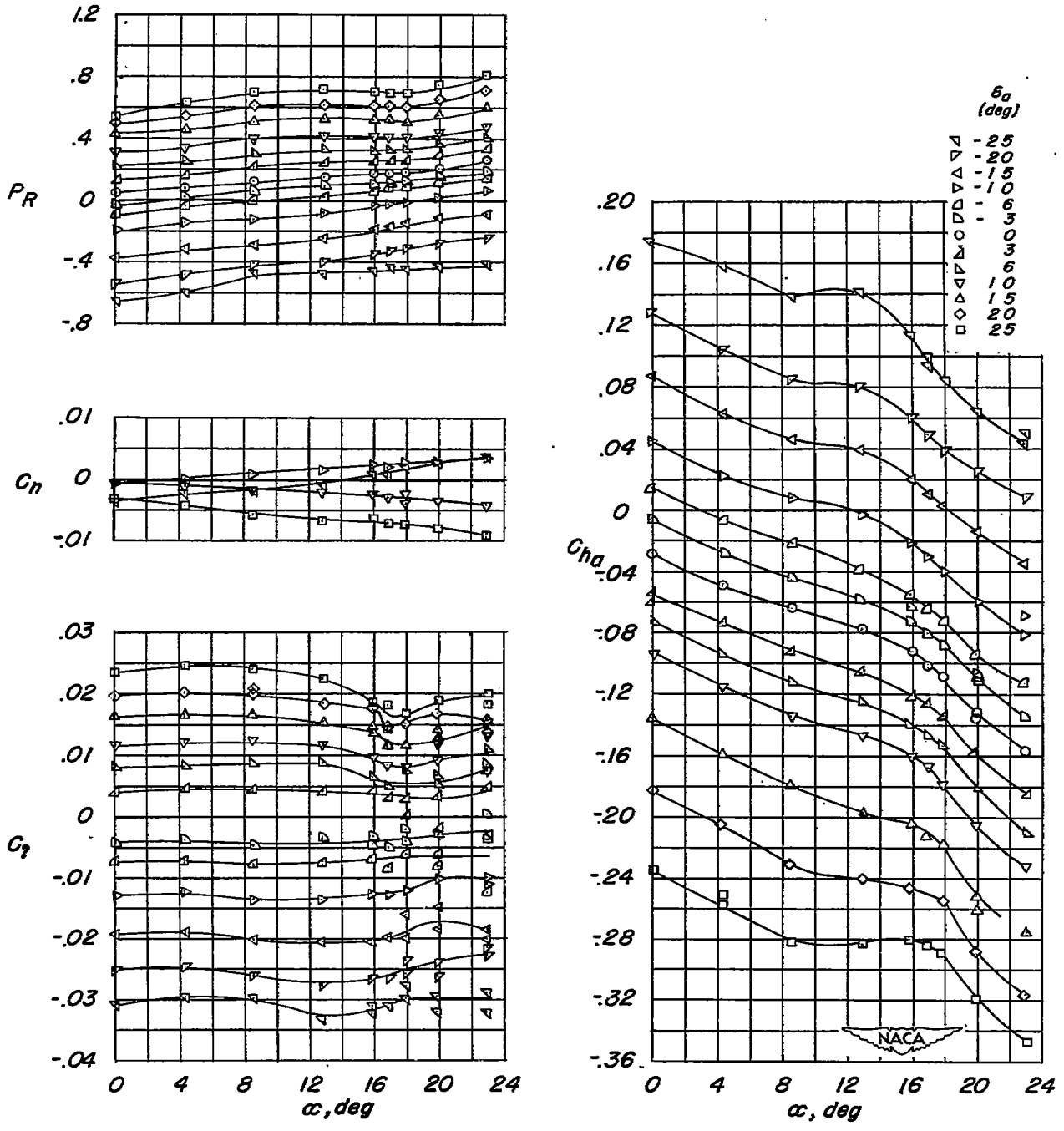

Figure 8.- Lateral-control characteristics of a 37° sweptback wing and aileron with leading-edge slat. $R = 6.8 \times 10^6$.

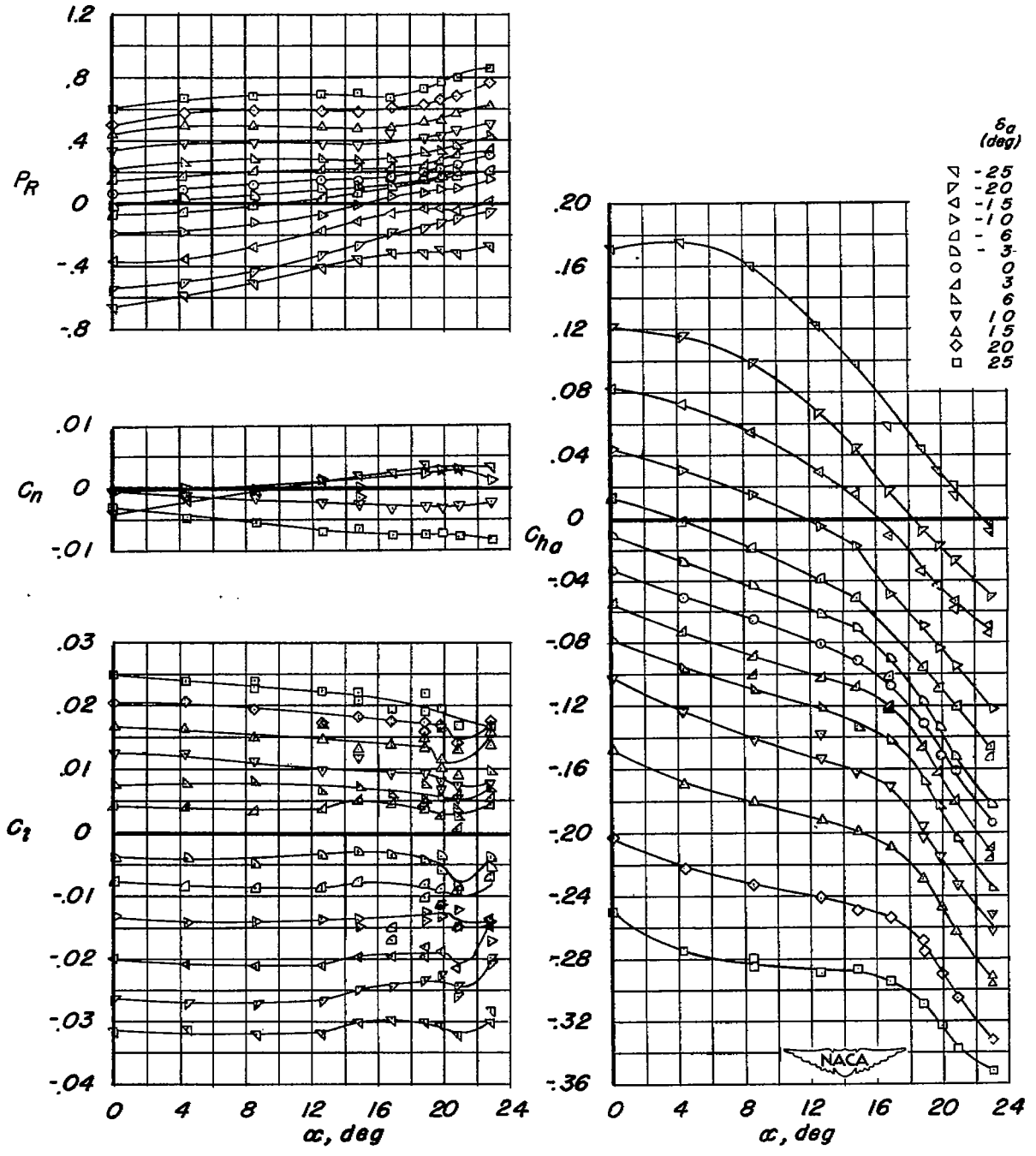

Figure 9.- Lateral-control characteristics of a 37° sweptback wing and aileron with drooped leading edge and upper-surface fence. $R = 6.8 \times 10^6$.

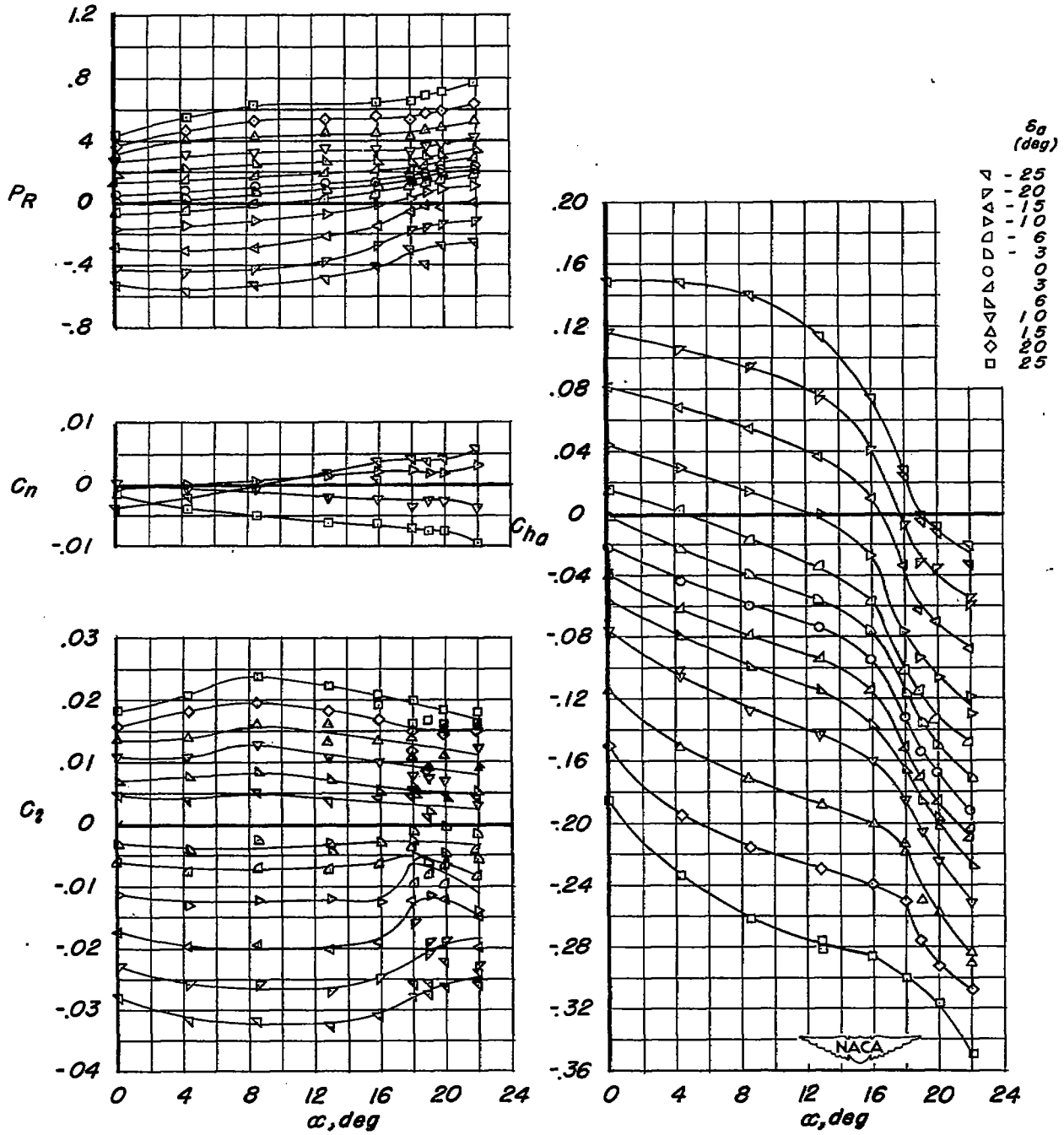

Figure 10.- Lateral-control characteristics of a 37° sweptback wing and aileron with leading-edge flap. $R = 6.8 \times 10^6$.

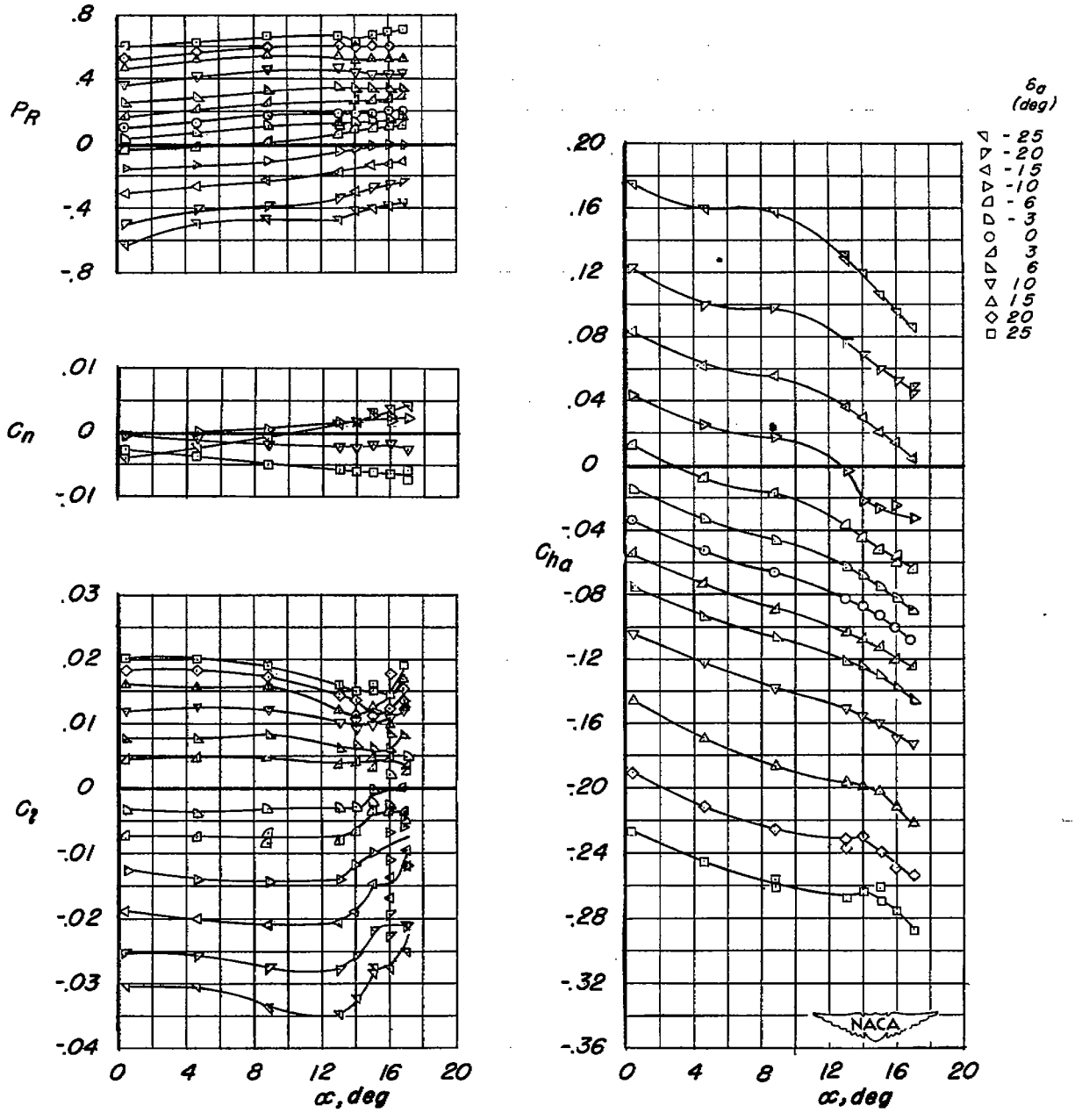

Figure 11.- Lateral-control characteristics of a 37° sweptback wing and aileron with leading-edge slat and semispan split flap. $R = 6.8 \times 10^6$.

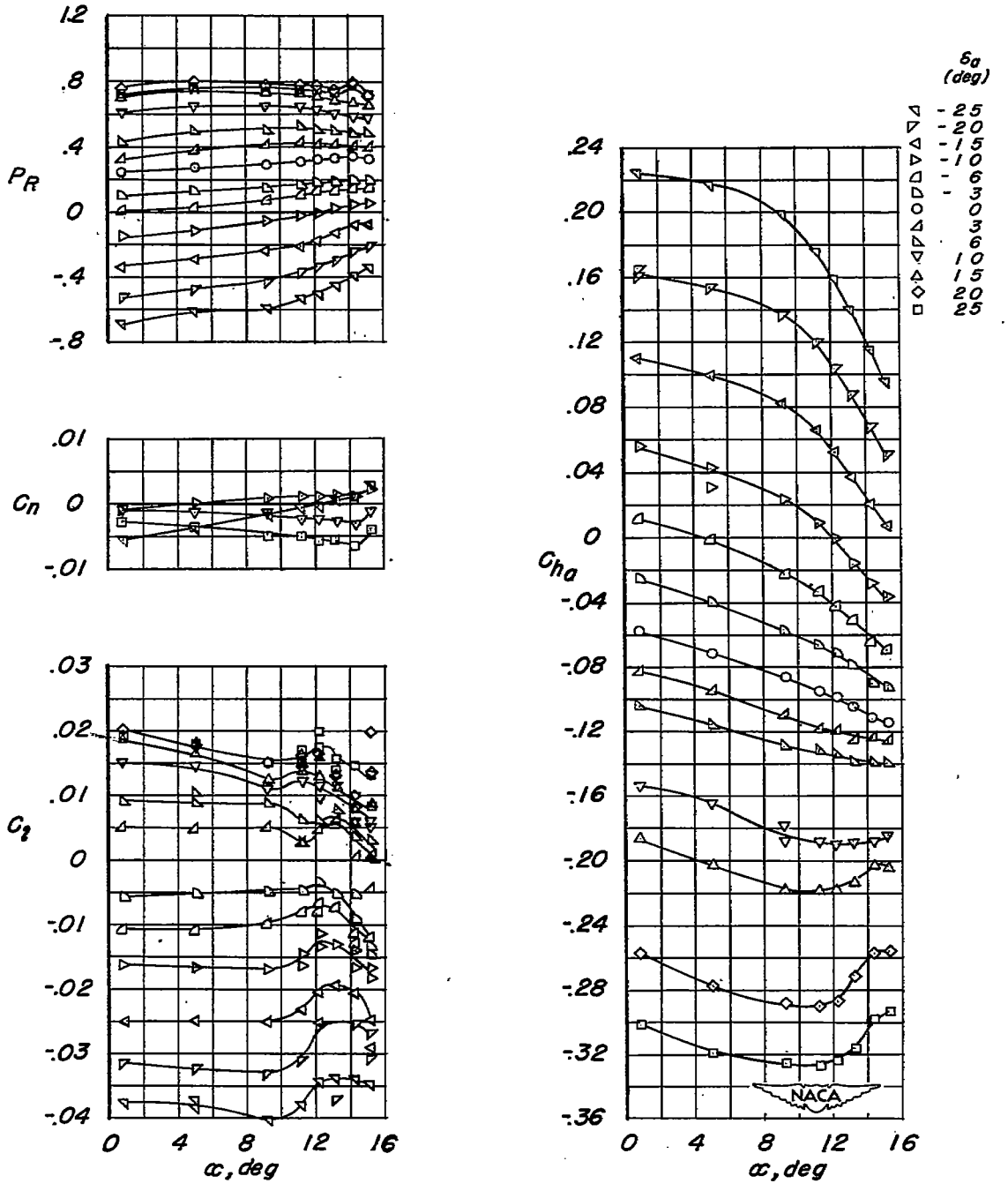

Figure 12.- Lateral-control characteristics of a 37° sweptback wing and aileron with leading-edge slat and semispan double slotted flap. $R = 6.8 \times 10^6$.

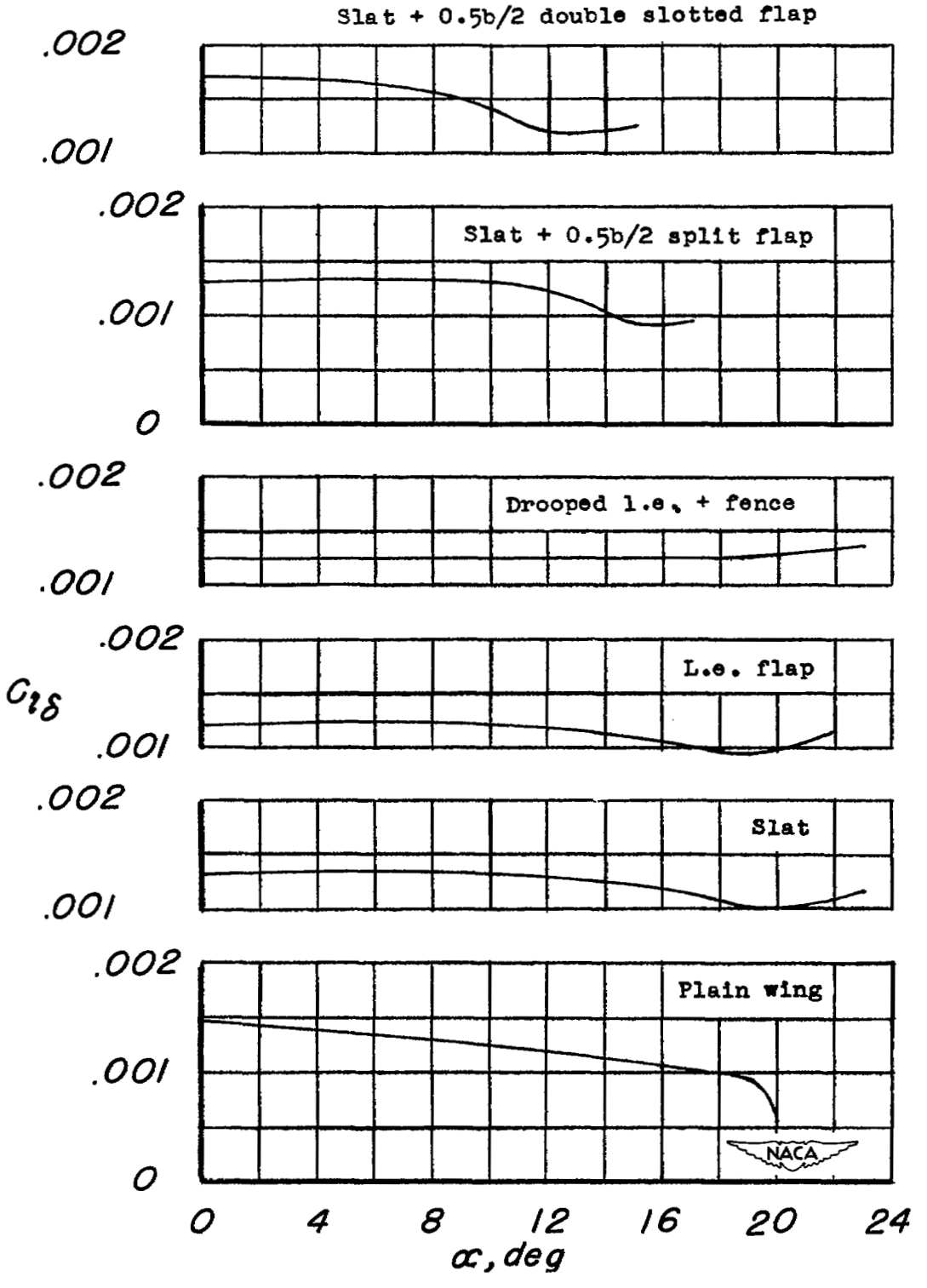

Figure 13.- Effects of the various leading-edge and trailing-edge devices on the aileron-effectiveness parameter C_{l_δ}.

$R = 6.8 \times 10^6$.

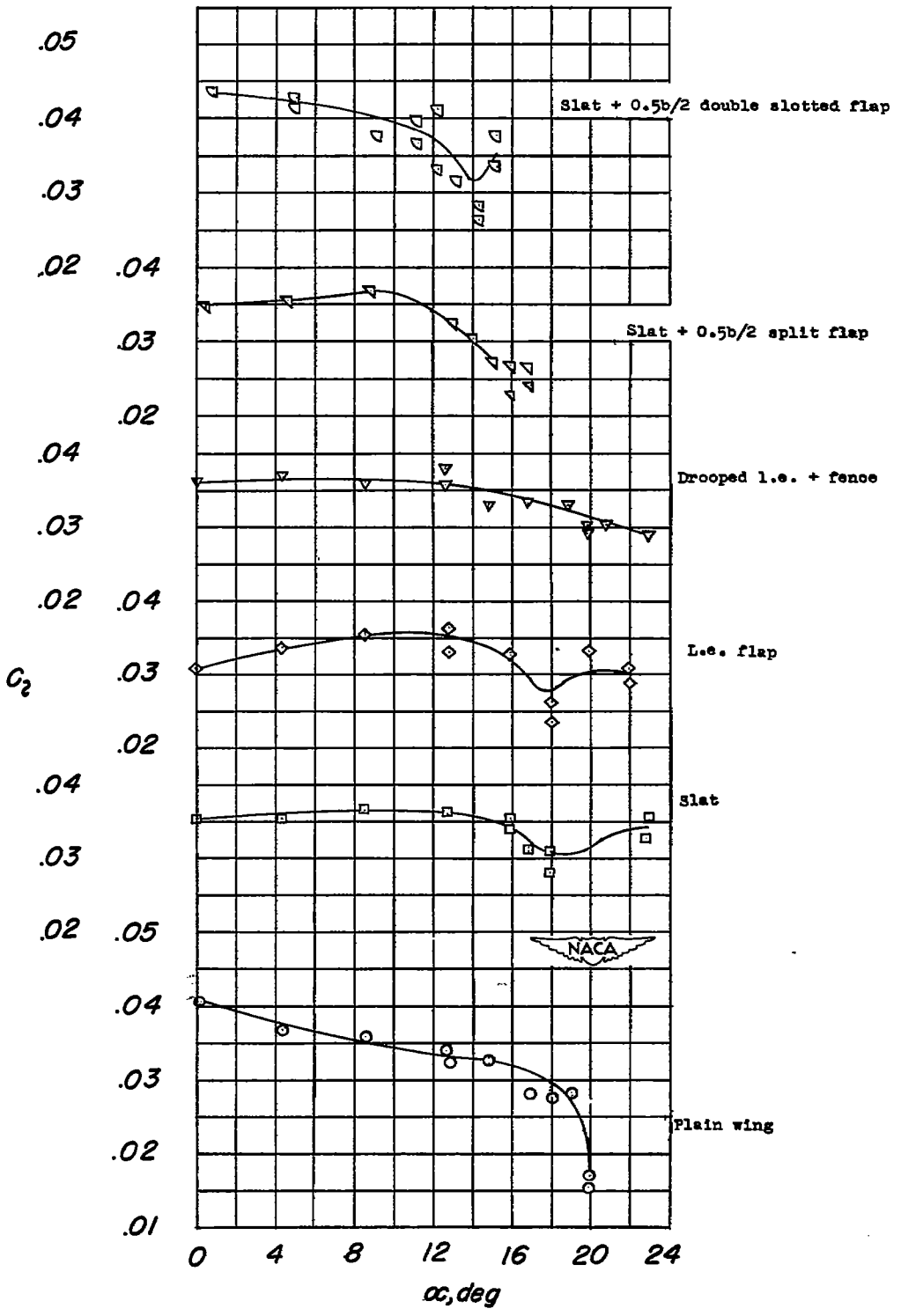

Figure 14.- Effect of various leading-edge and trailing-edge devices on the rolling-moment coefficient for a total aileron deflection of 30° on a 37° sweptback wing. $R = 6.8 \times 10^6$.

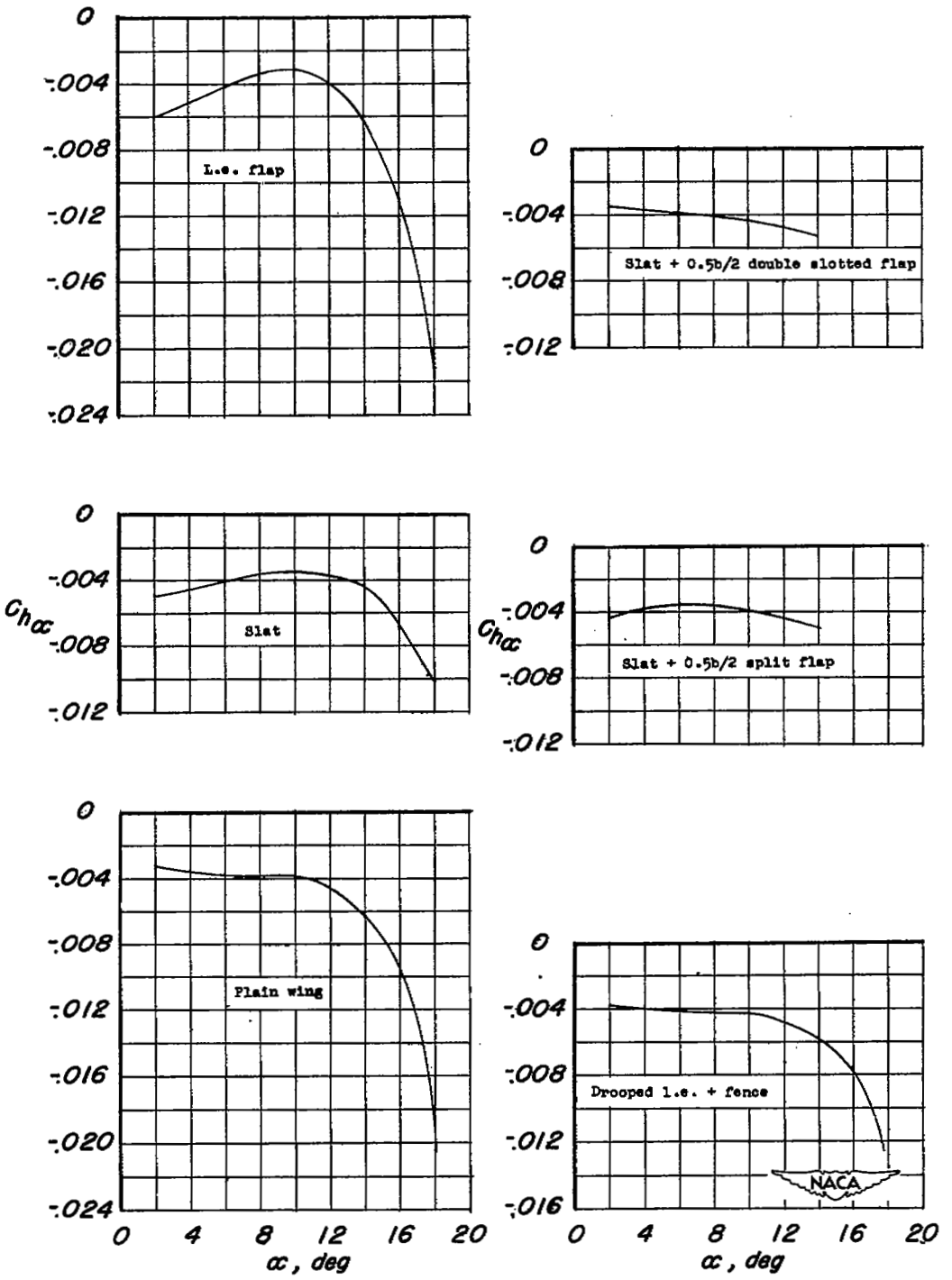

(a) C_{h_α}.

Figure 15.– Effects of the various leading-edge and trailing-edge devices on the aileron parameters C_{h_α}, P_{R_α}, C_{h_δ}, and P_{R_δ}, for an aileron on a 37° sweptback wing. $R = 6.8 \times 10^6$.

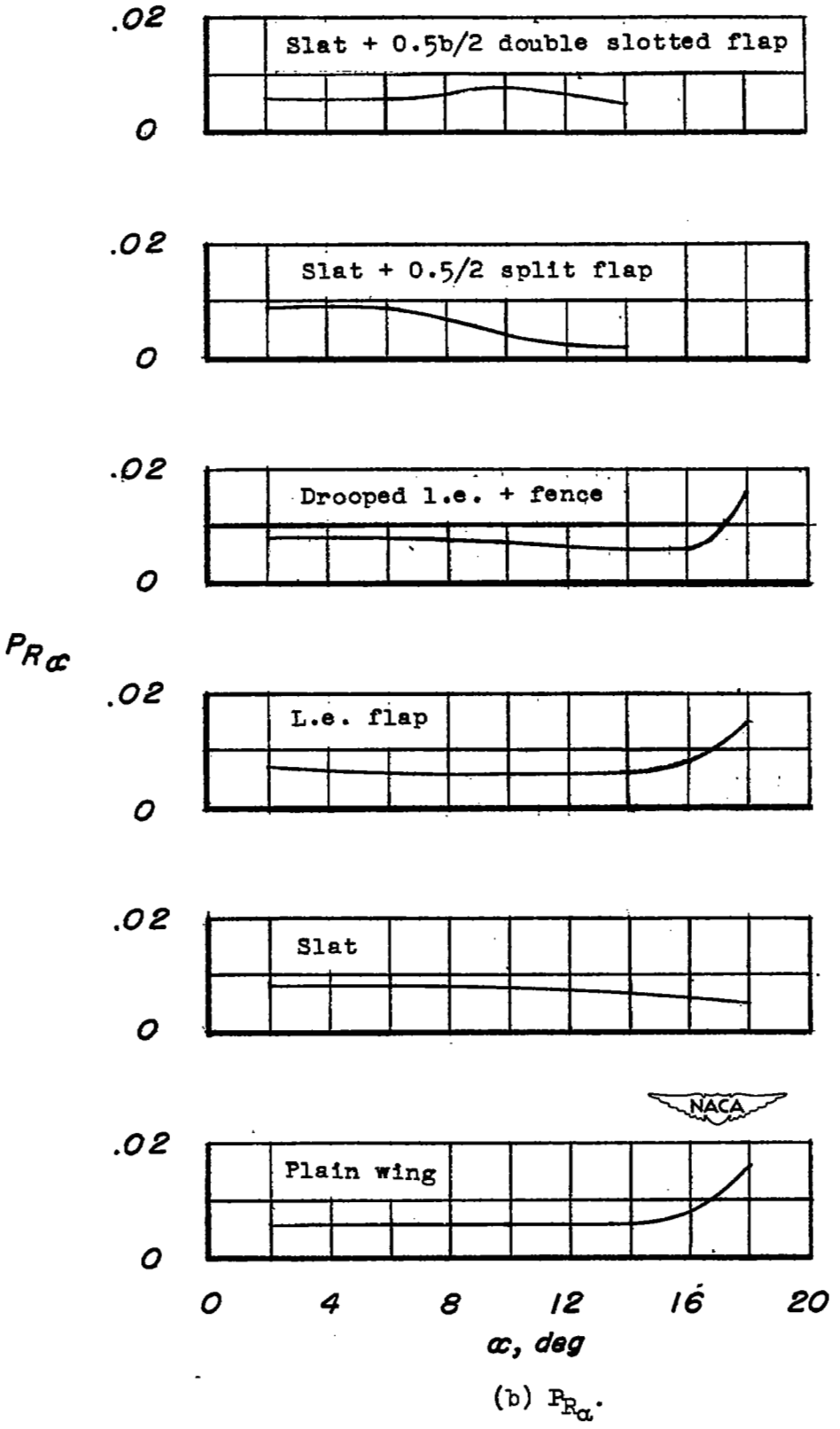

(b) P_{R_α}.

Figure 15.- Continued.

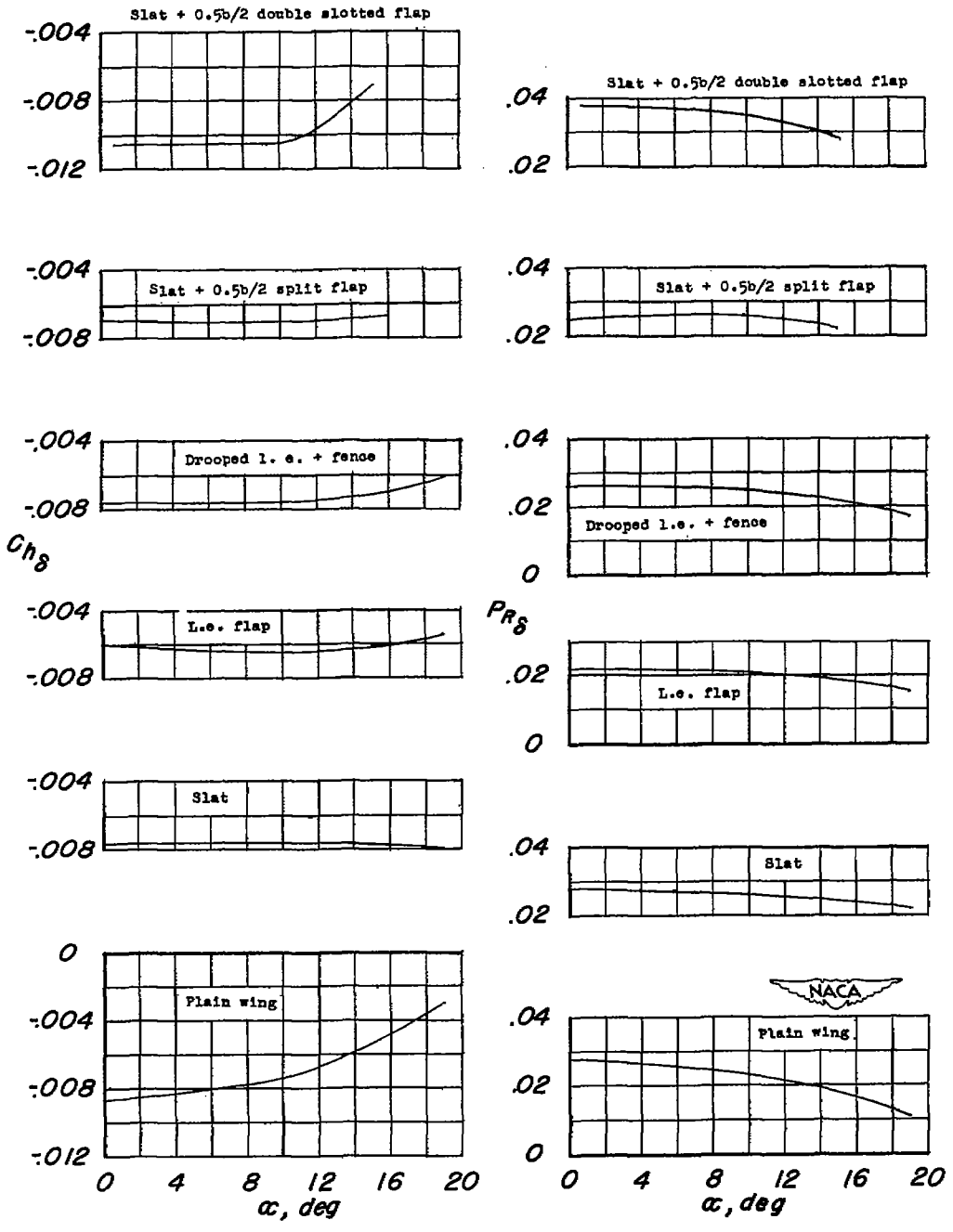

(c) C_{h_δ}. (d) P_{R_δ}.

Figure 15.- Concluded.

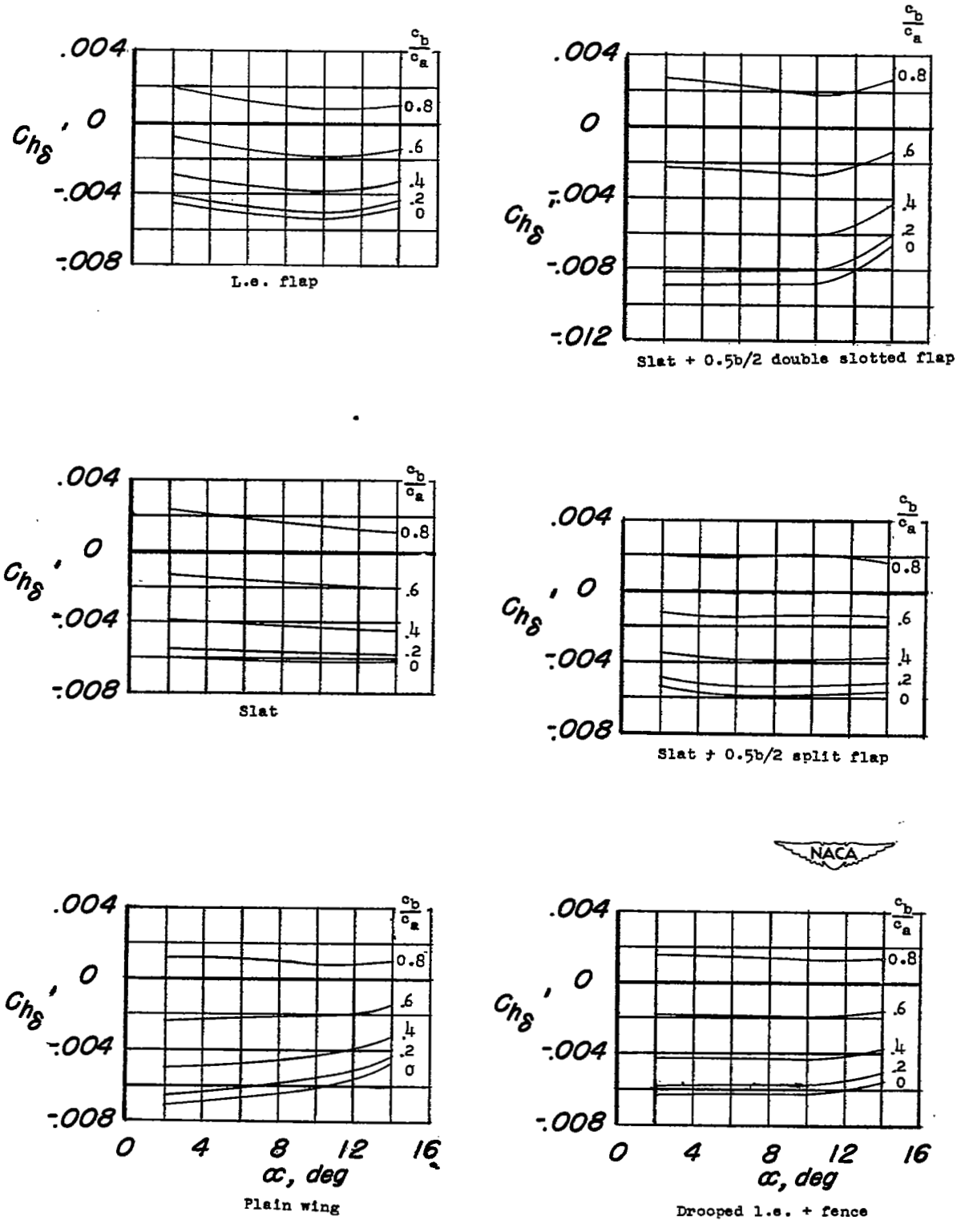

Figure 16.- Effects of a sealed internal balance on C_{h_δ}' for the aileron.

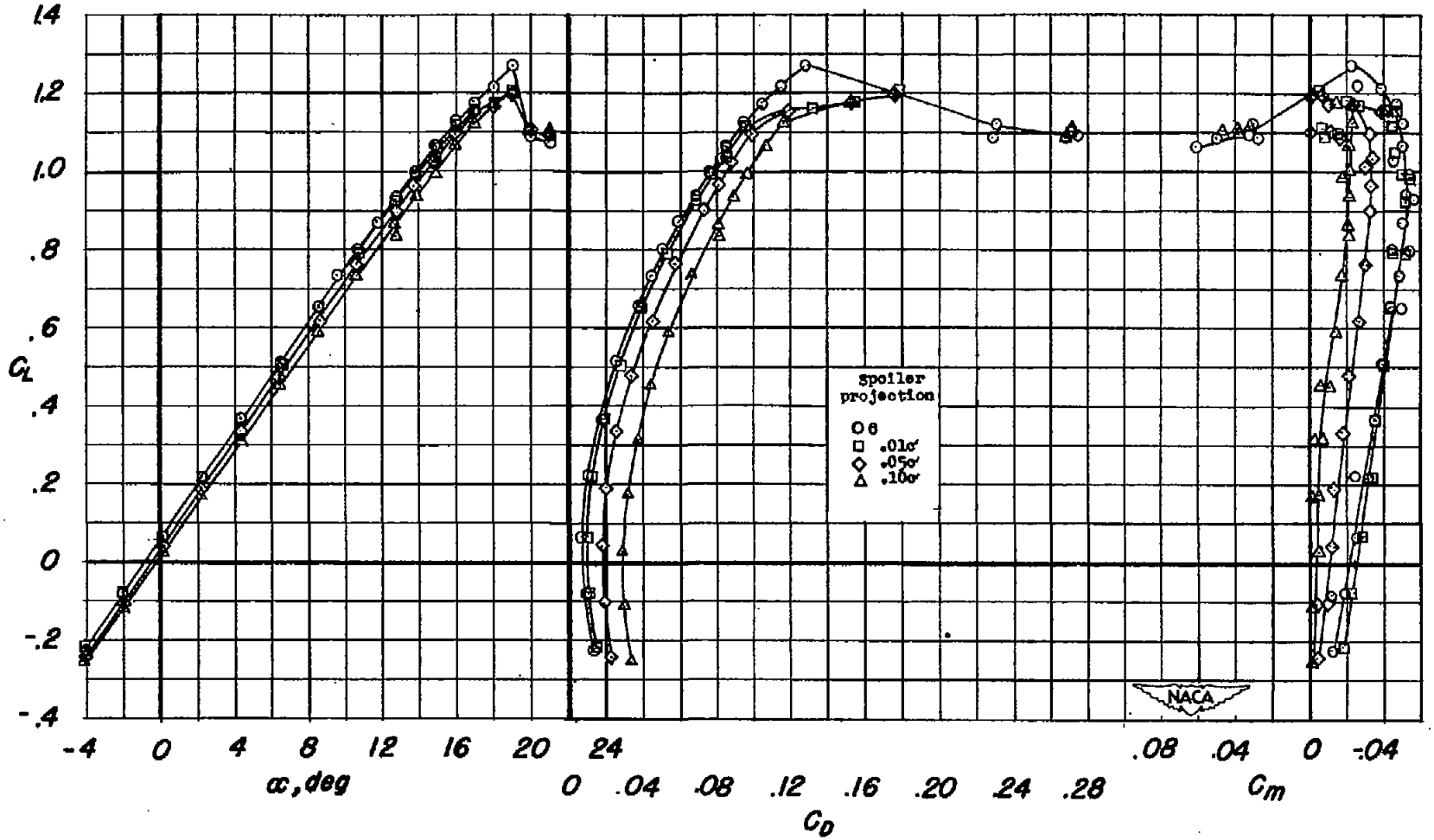

(a) Lift, drag, and pitching moment.

Figure 17.- Effects of half-span plain spoilers at 0.65c' on the aerodynamic characteristics of a 37° sweptback wing. $R = 6.8 \times 10^6$.

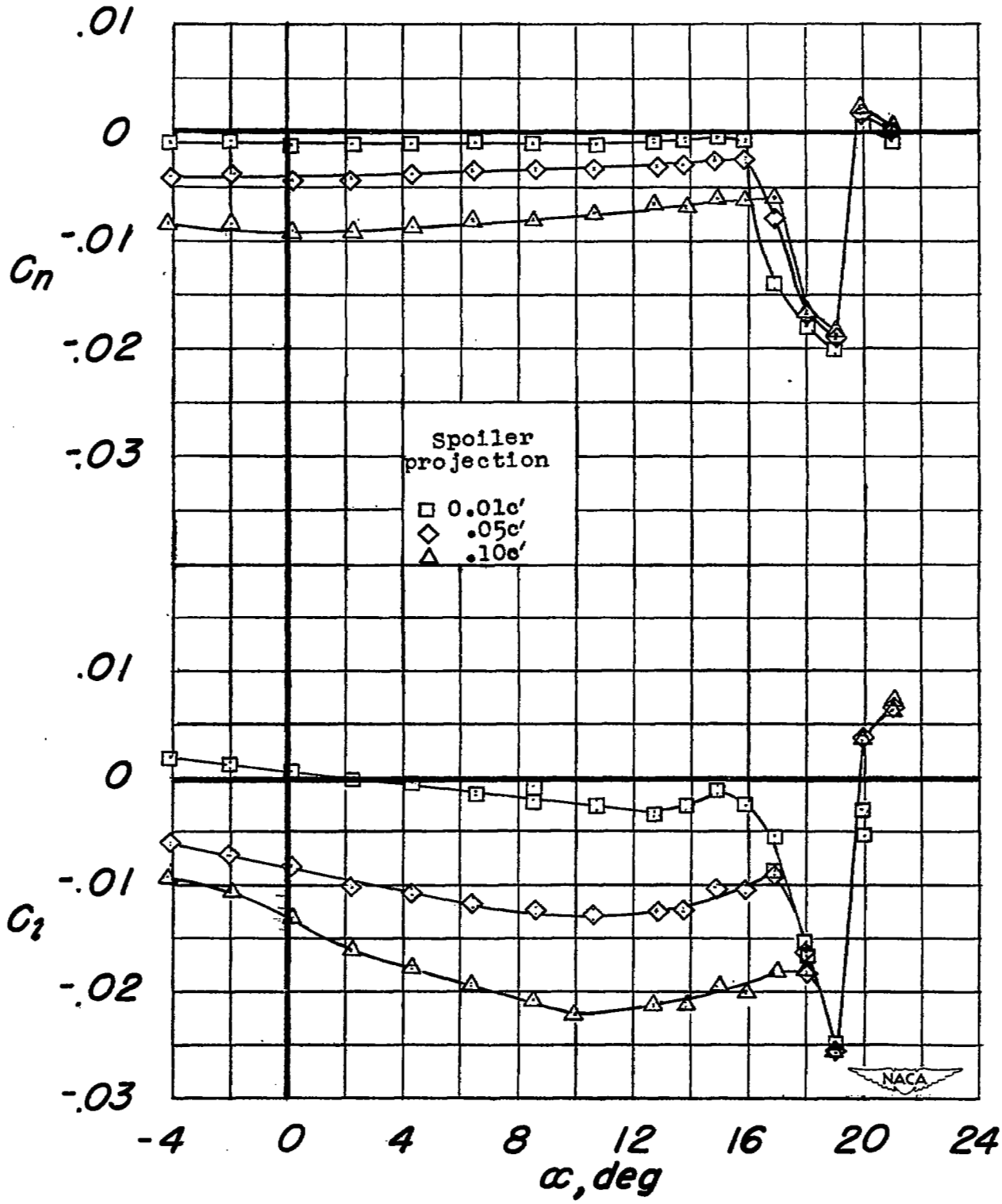

(b) Rolling moment and yawing moment.

Figure 17.- Concluded.

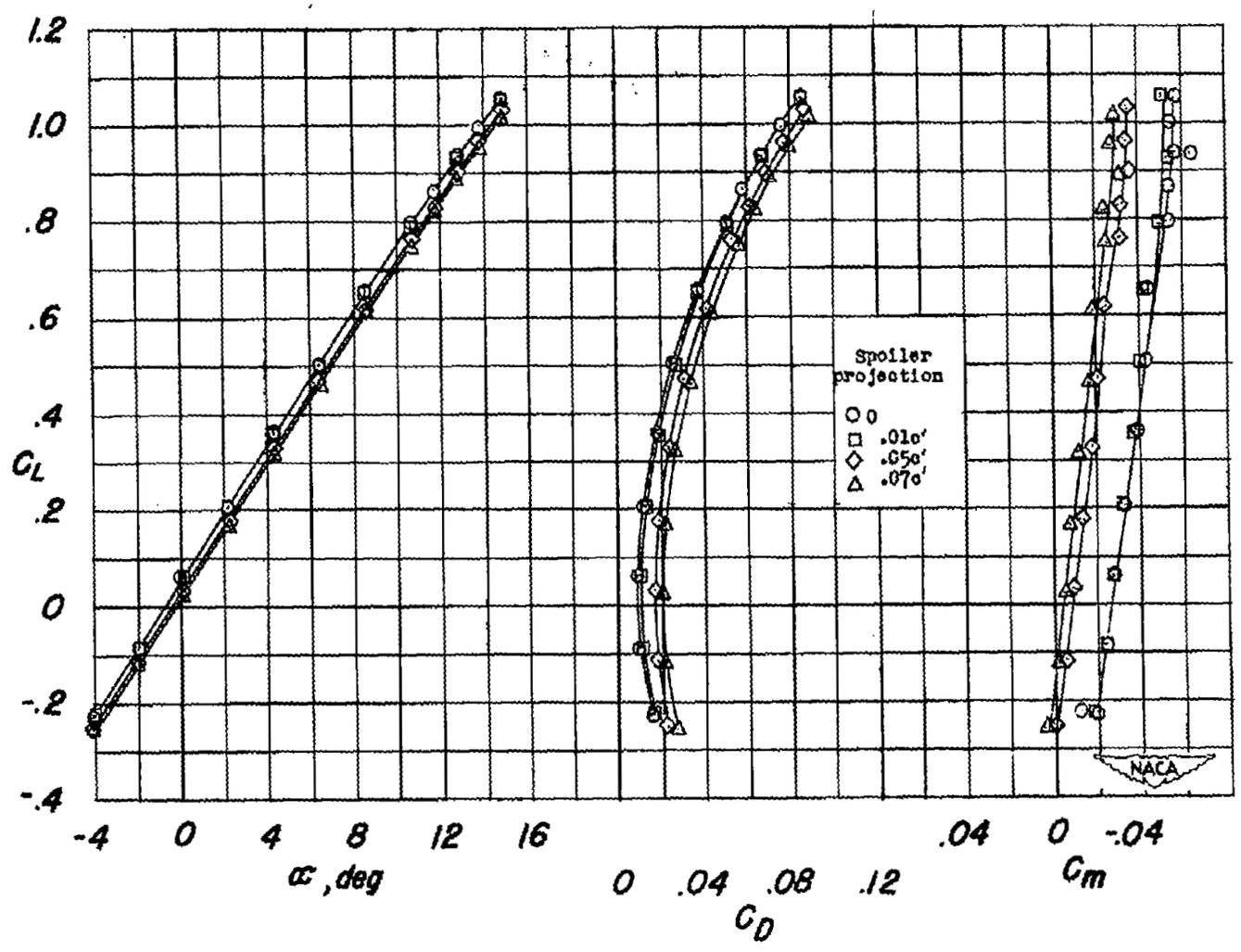

(a) Lift, drag, and pitching moment.

Figure 18.- Effects of half-span plain spoilers at 0.75c' on the aerodynamic characteristics of a 37° sweptback wing. $R = 6.8 \times 10^6$.

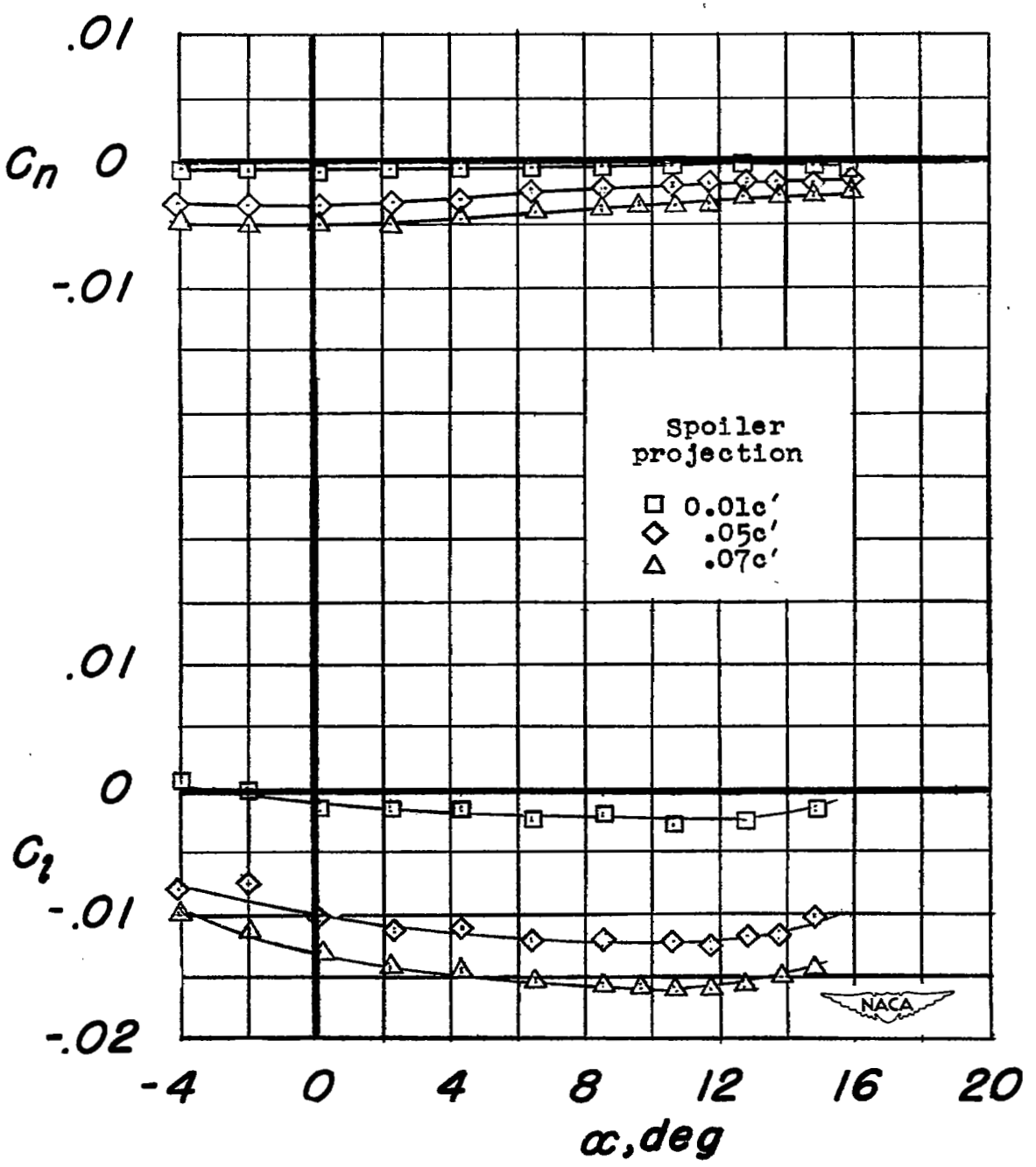

(b) Rolling moment and yawing moment.

Figure 18.- Concluded.

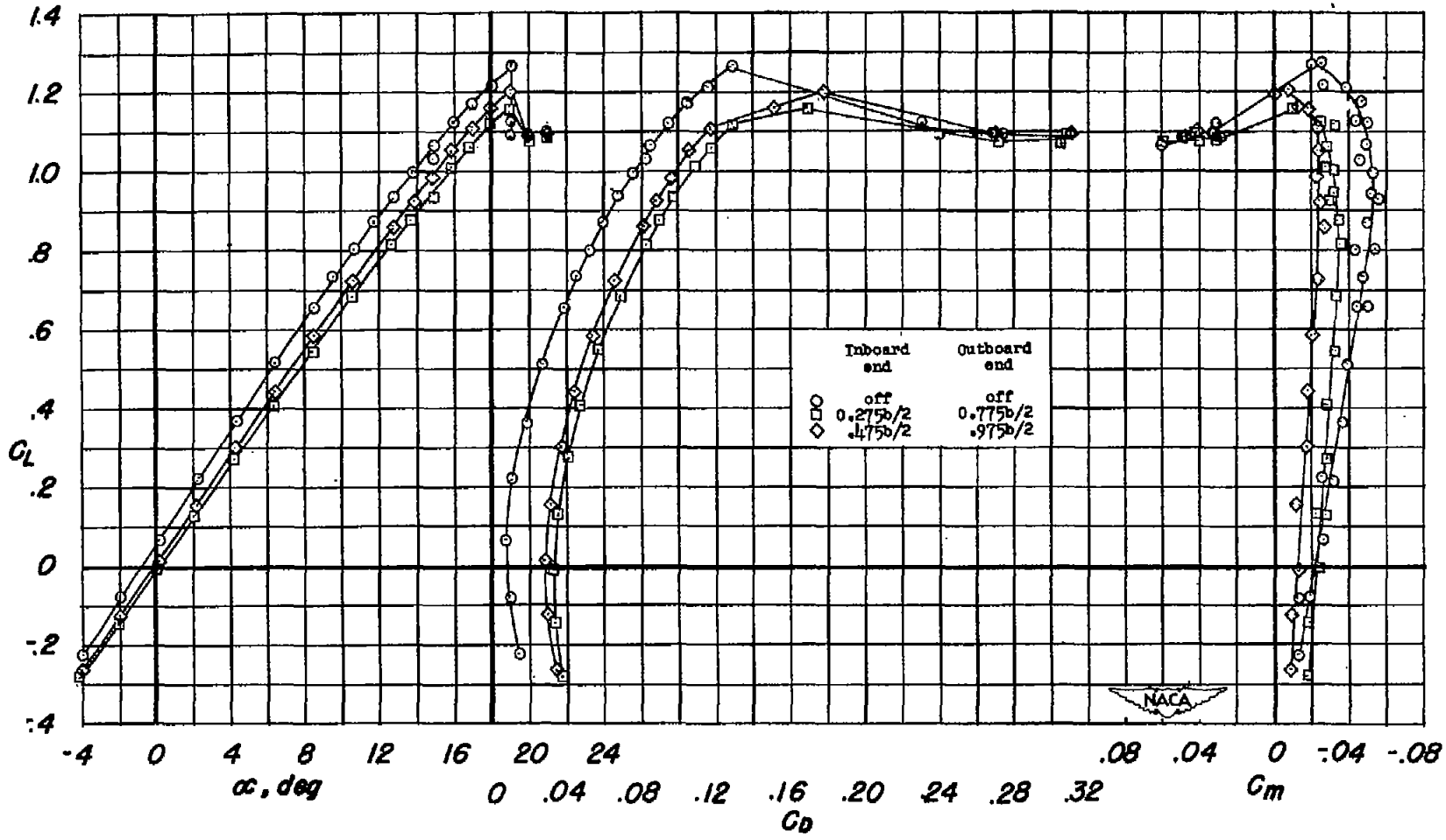

(a) Lift, drag, and pitching moment.

Figure 19.– Effects of step spoilers at 0.65c' on the aerodynamic characteristics of a 37° sweptback wing. Spoiler projection 0.10c'; R = 6.8×10^6.

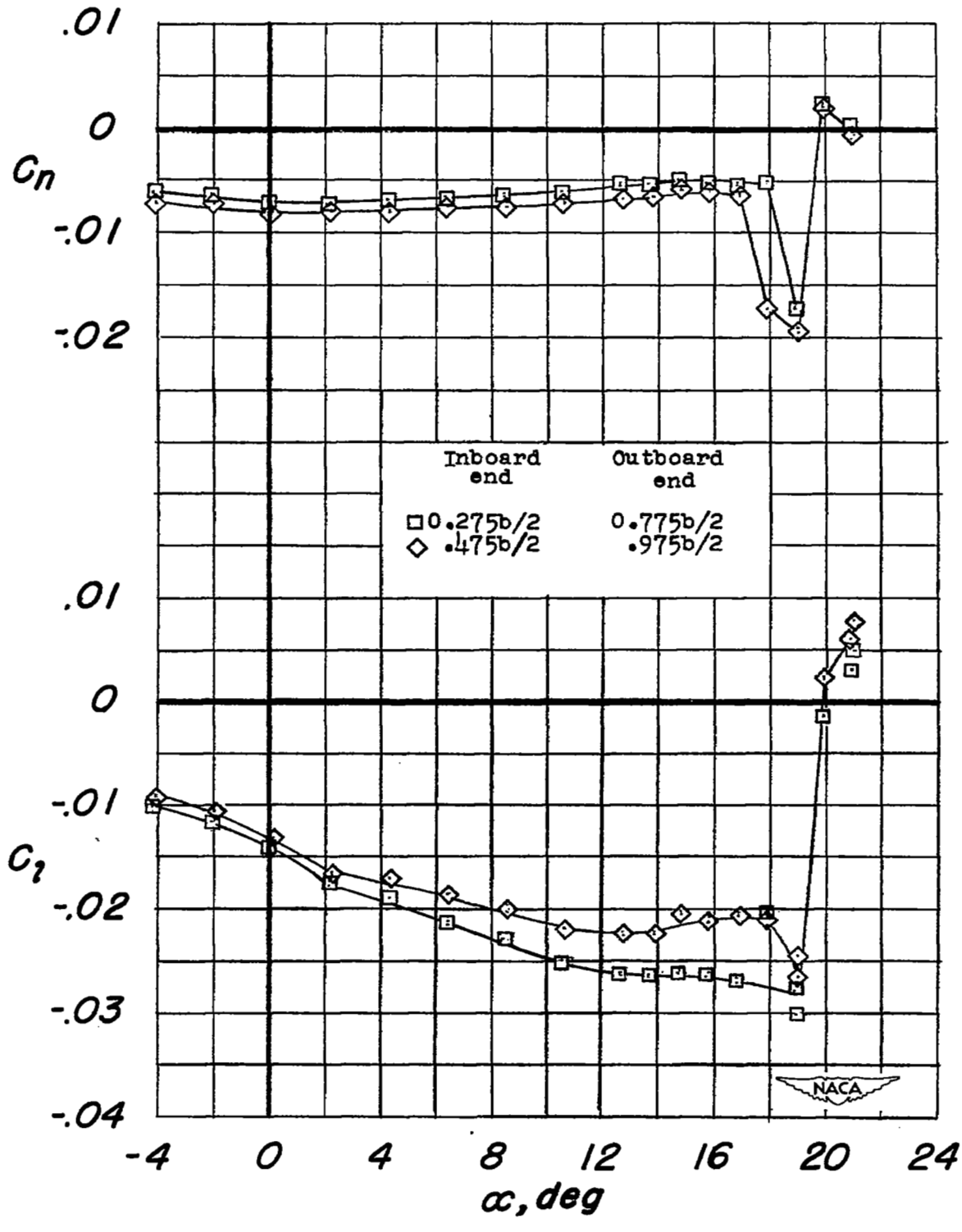

(b) Rolling moment and yawing moment.

Figure 19.- Concluded.

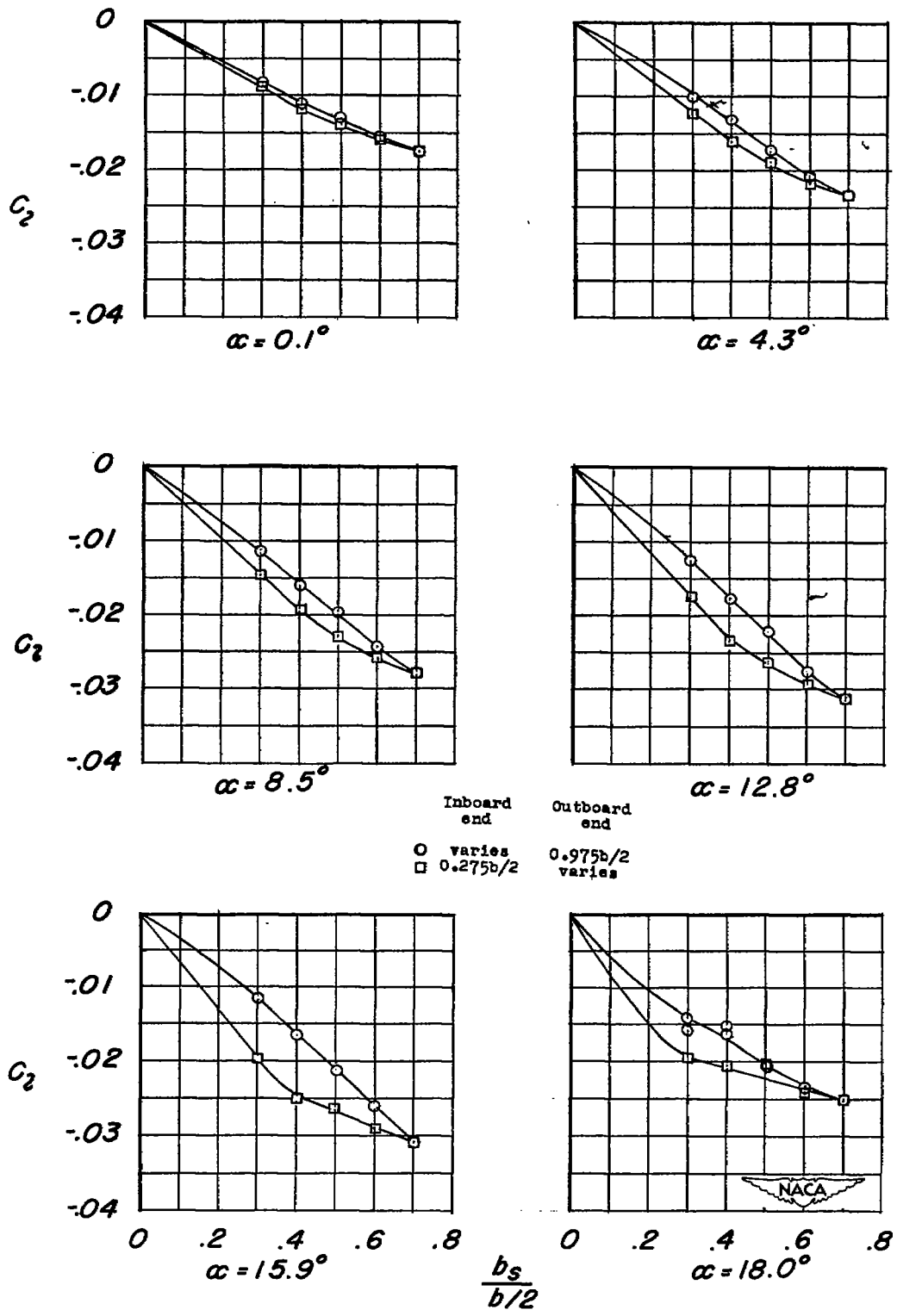

Figure 20.– Variation of rolling-moment coefficient with span of a step spoiler at 0.65c' on a 37° sweptback wing. Spoiler projection 0.10c'; $R = 6.8 \times 10^6$.

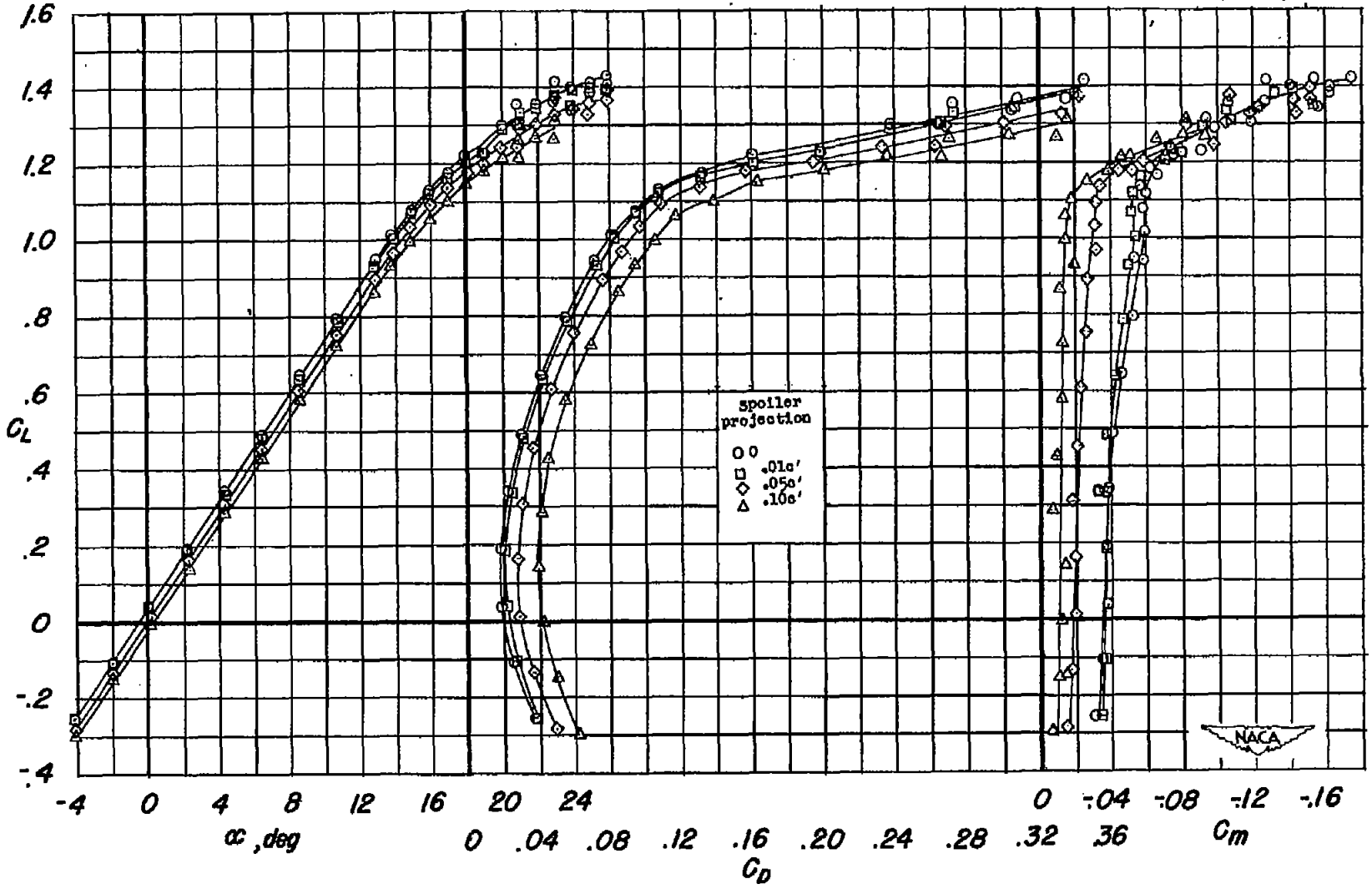

(a) Lift, drag, and pitching moment.

Figure 21.- Effects of half-span plain spoilers at 0.65c' on the aerodynamic characteristics of 37° sweptback wing with leading-edge slat. $R = 6.8 \times 10^6$.

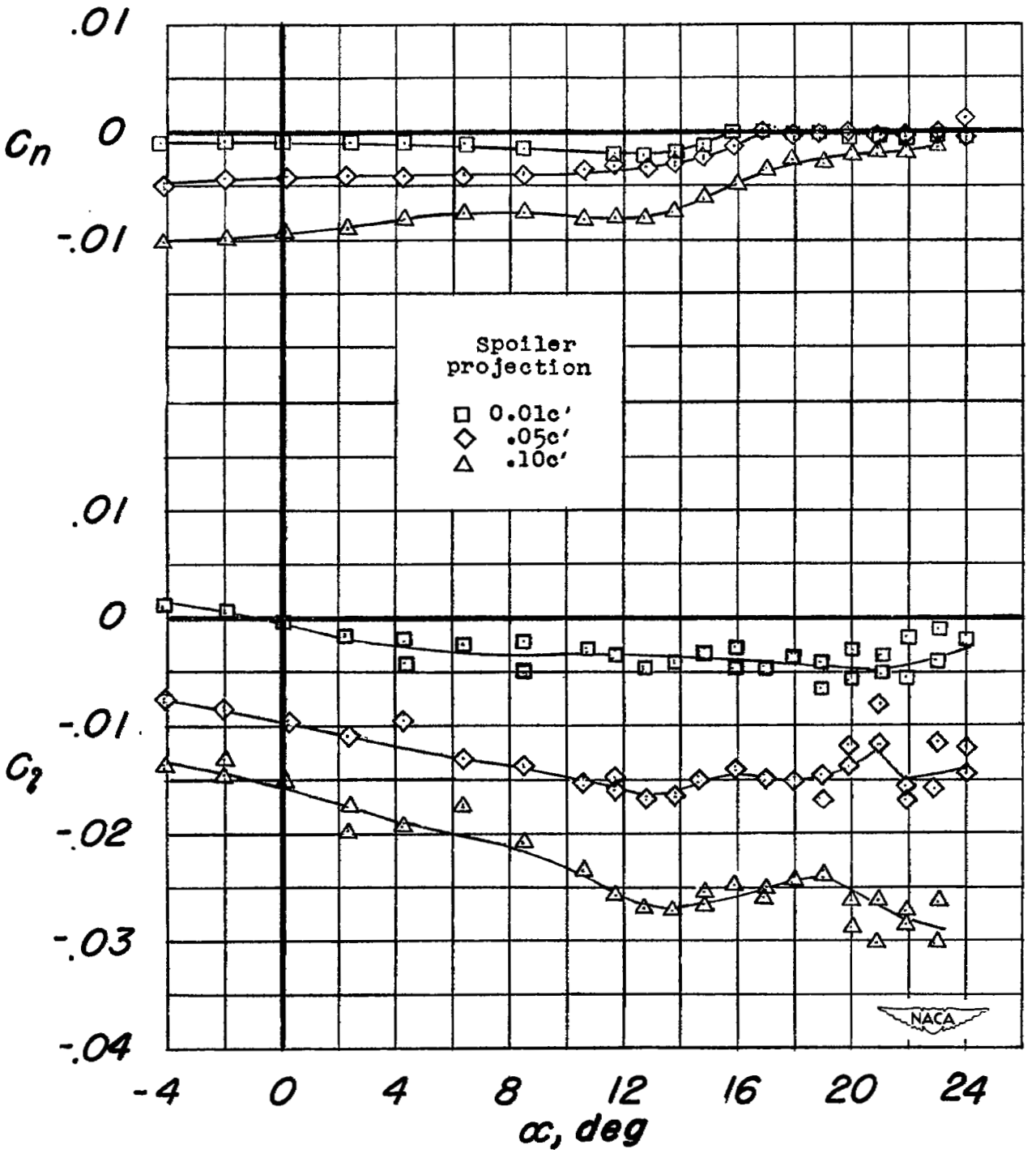

(b) Rolling moment and yawing moment.

Figure 21.- Concluded.

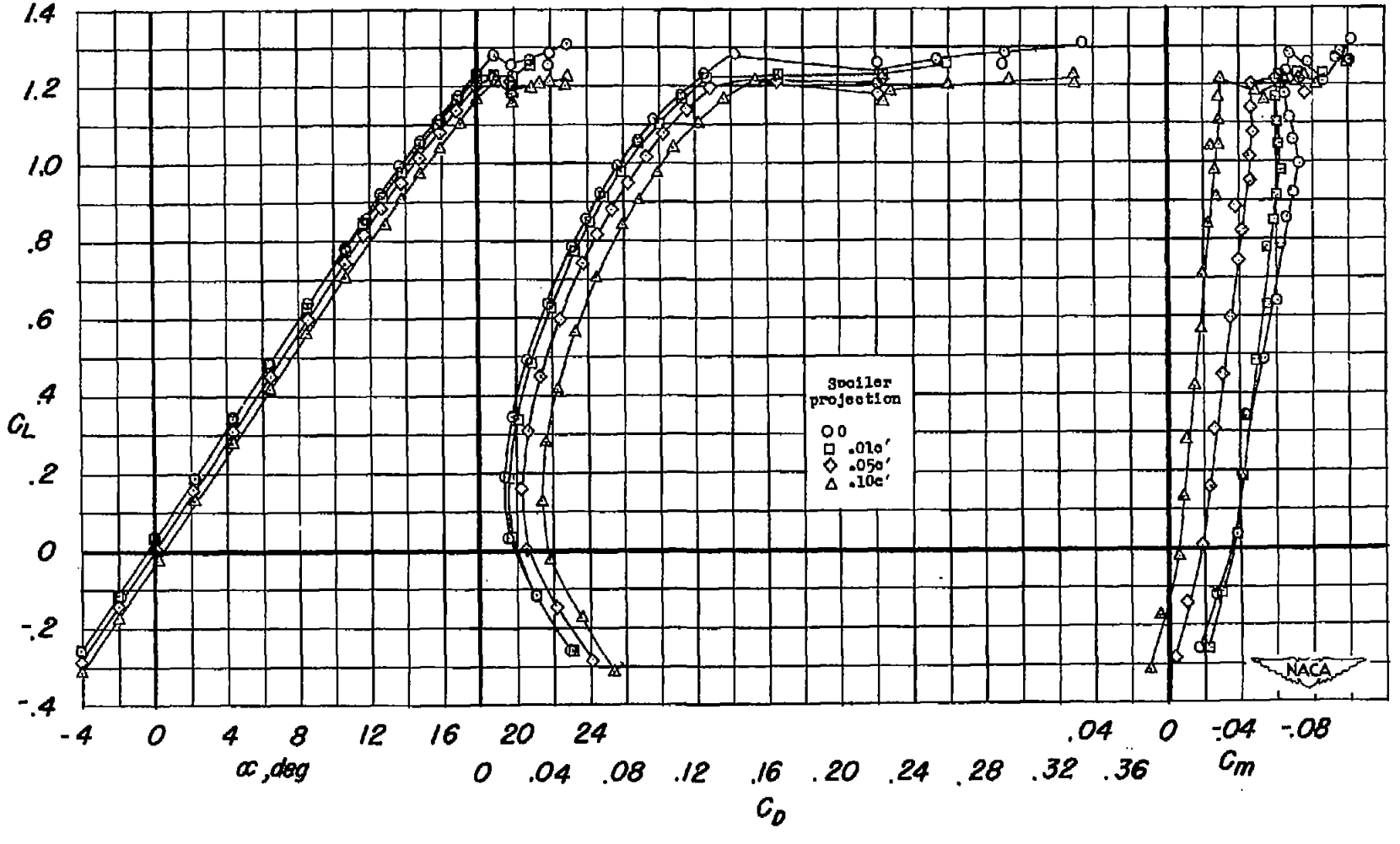

(a) Lift, drag, and pitching moment.

Figure 22.- Effects of half-span spoilers at 0.65c' on the aerodynamic characteristics of a 37° sweptback wing with drooped leading edge and upper-surface fence. R = 6.8×10^6.

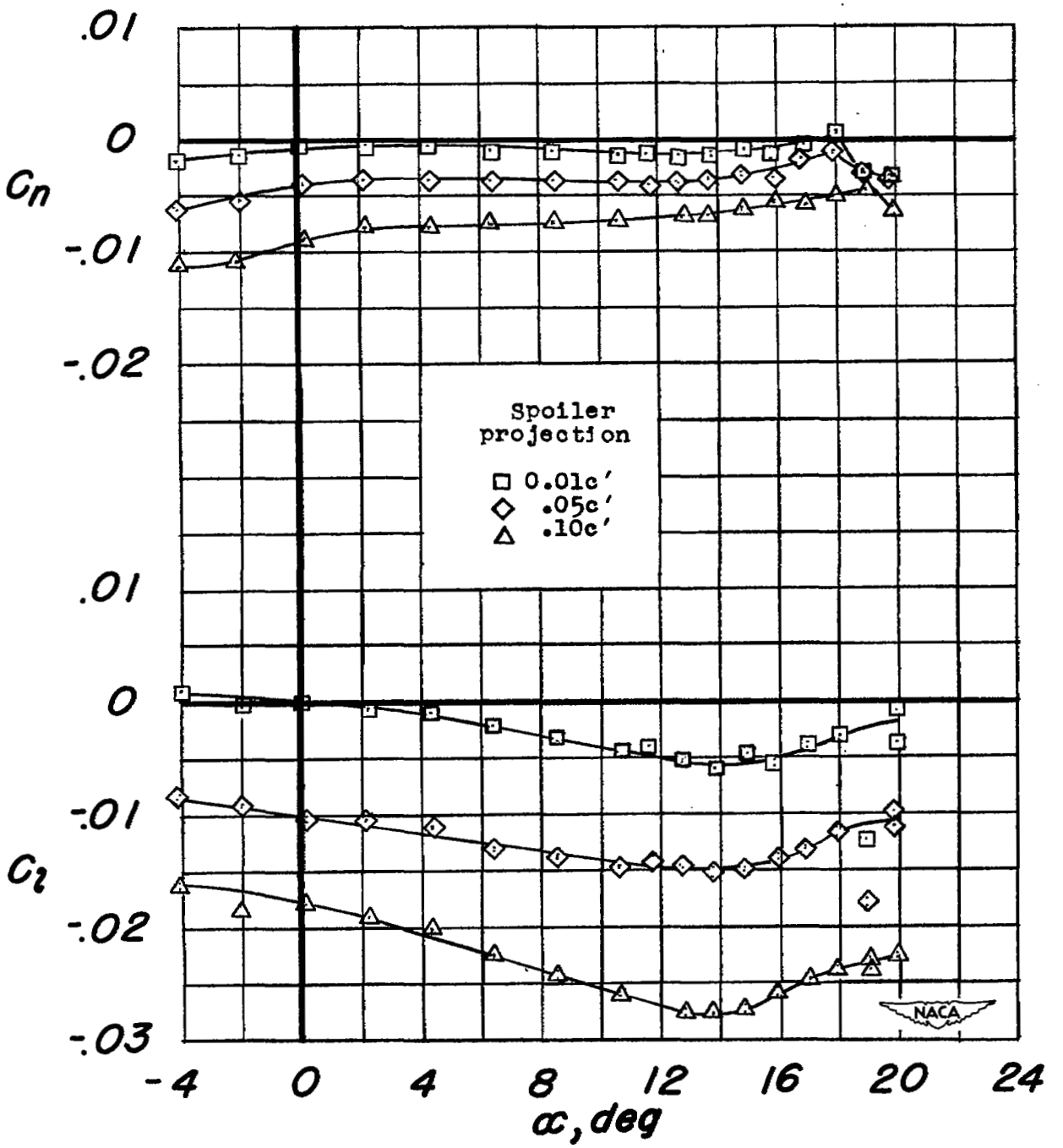

(b) Rolling moment and yawing moment.

Figure 22.- Concluded.

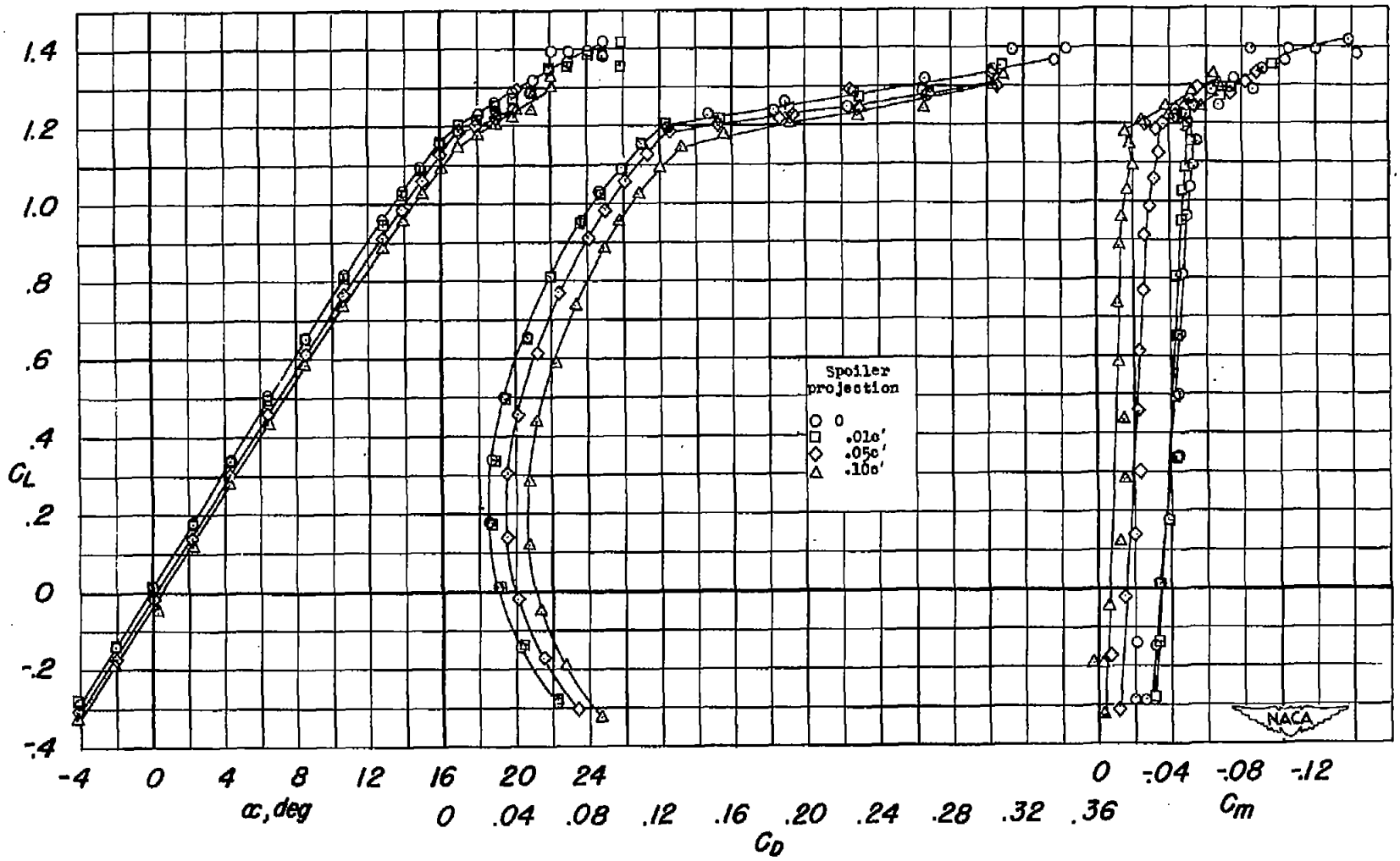

(a) Lift, drag, and pitching moment.

Figure 23.- Effects of half-span plain spoilers at 0.65c' on the aerodynamic characteristics of 37° sweptback wing with leading-edge flap. $R = 6.8 \times 10^6$.

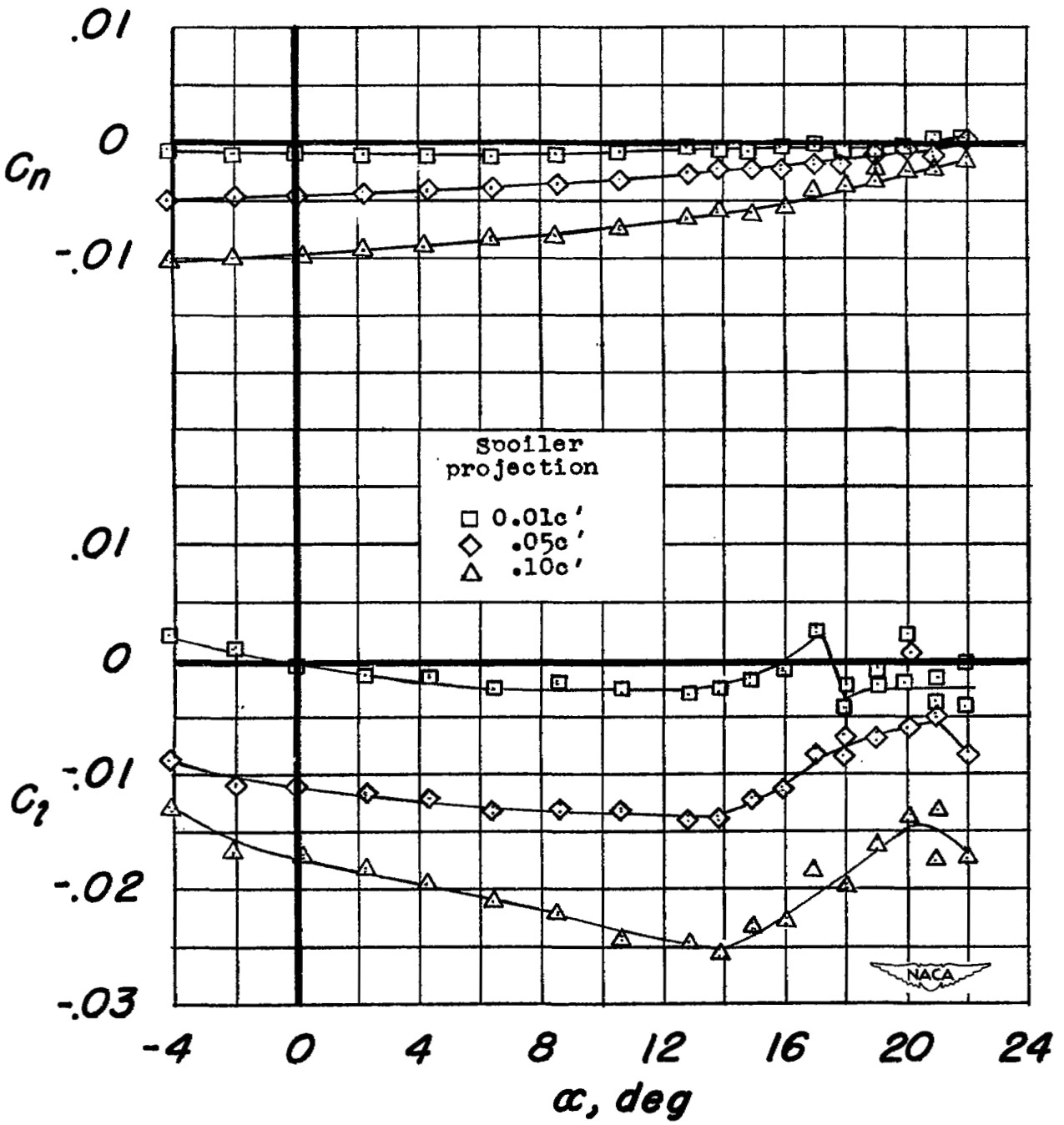

(b) Rolling moment and yawing moment.

Figure 23.- Concluded.

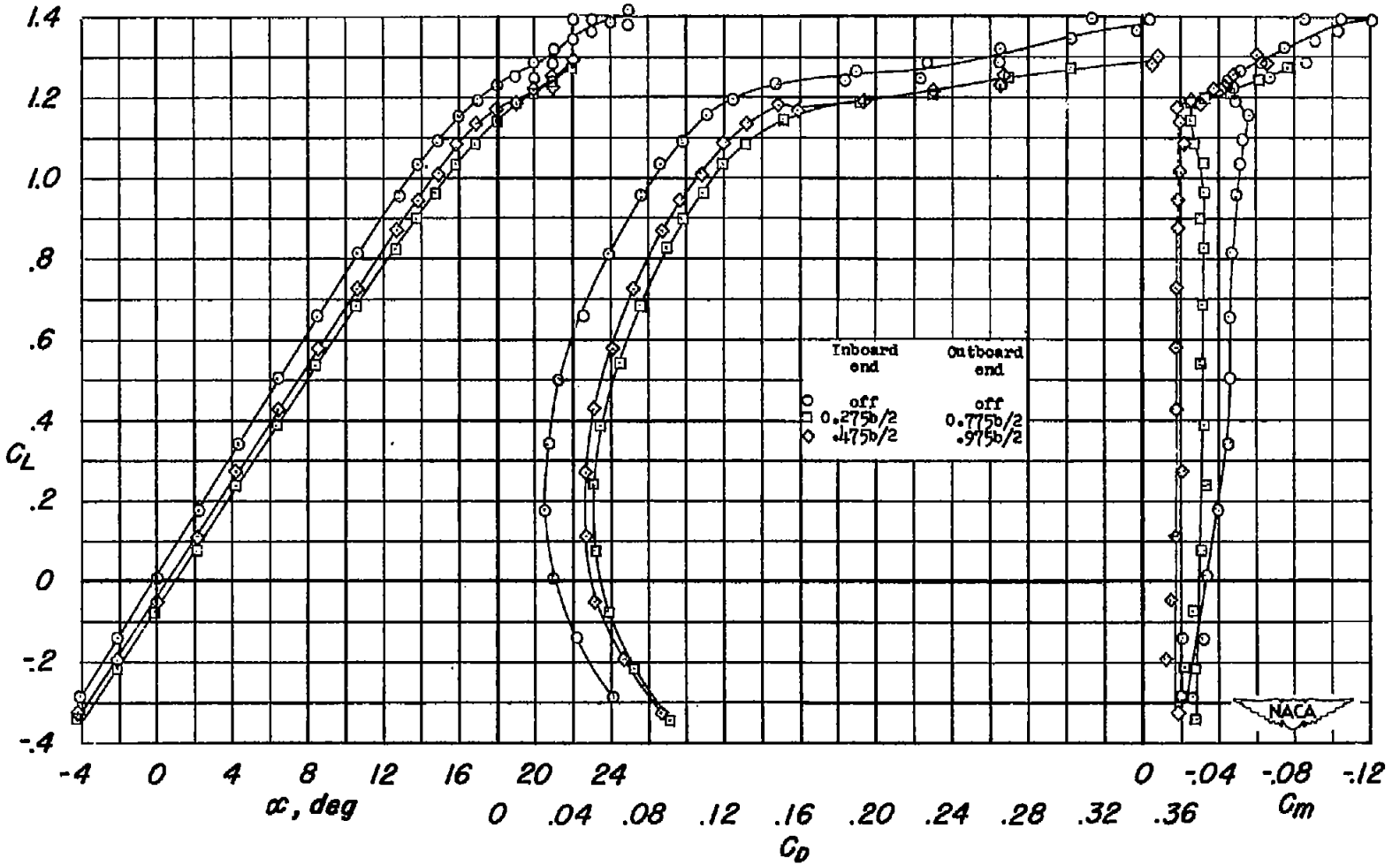

(a) Lift, drag, and pitching moment.

Figure 24.- Effects of step spoilers at 0.65c' on the aerodynamic characteristics of a 37° sweptback wing with leading-edge flap. Spoiler projection 0.10c'; R = 6.8×10^6.

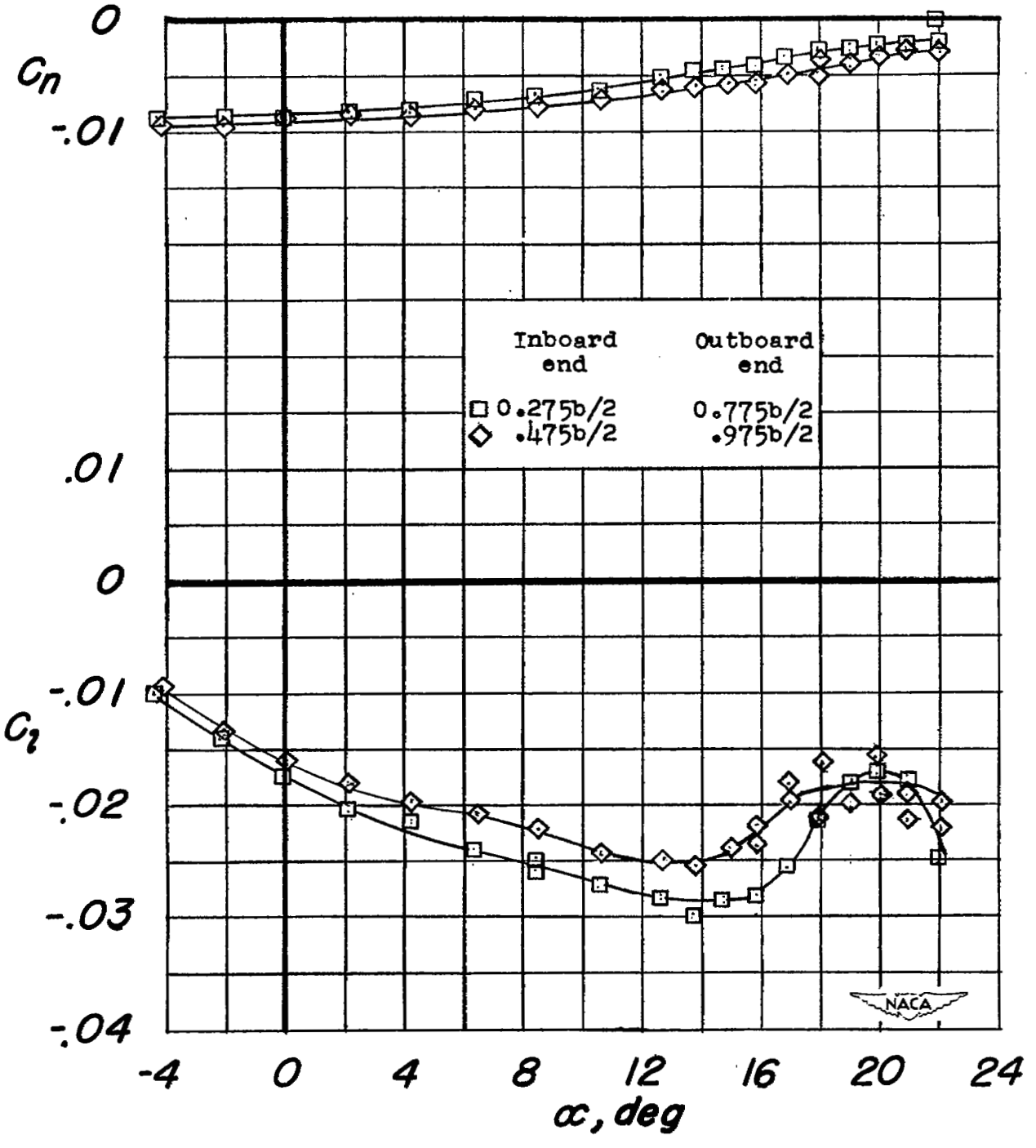

(b) Rolling moment and yawing moment.

Figure 24.- Concluded.

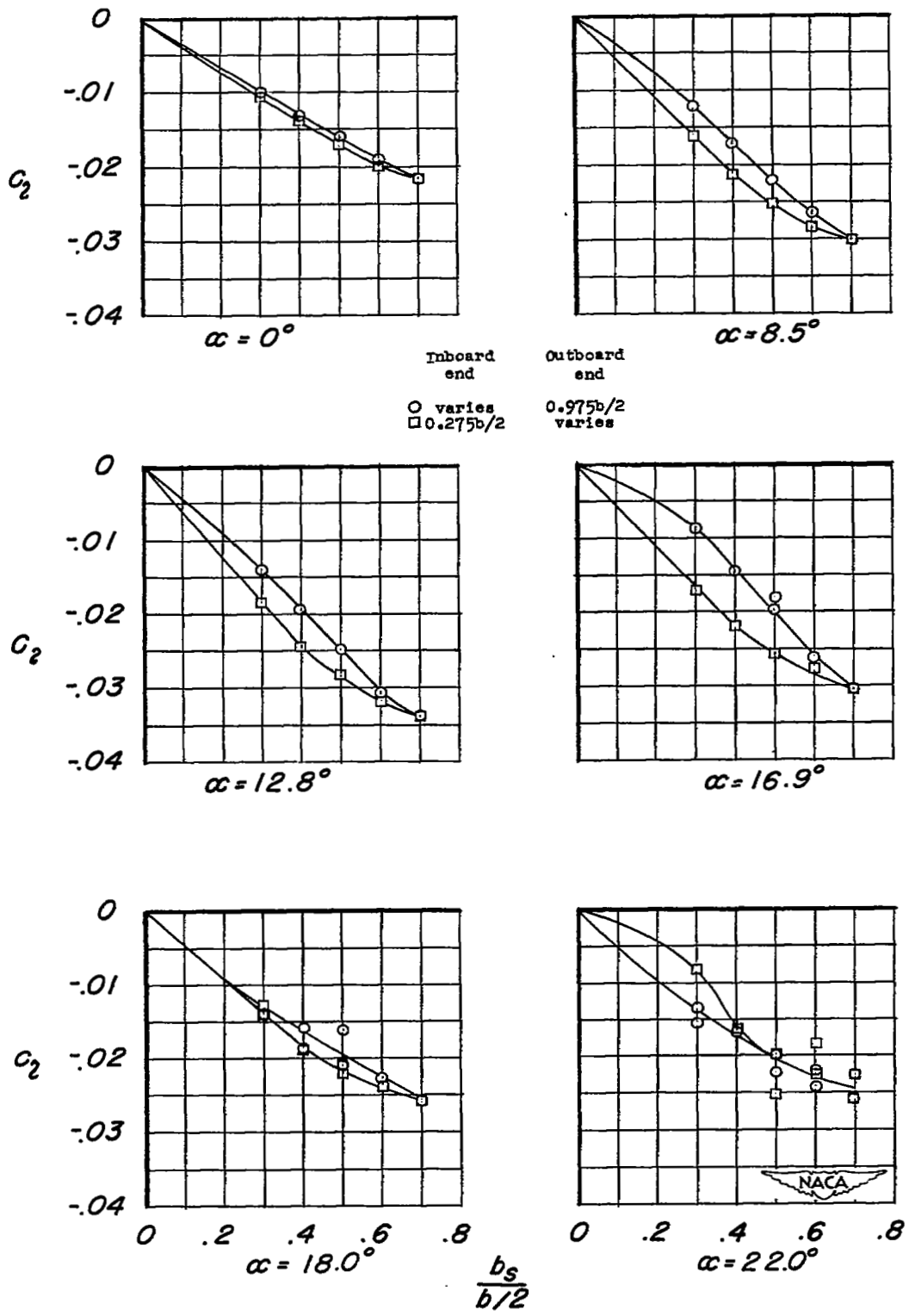

Figure 25.- Variation of rolling-moment coefficient with span of a step spoiler at 0.65c' on a 37° sweptback wing with leading-edge flap. Spoiler projection 0.10c'; R = 6.8×10^6.

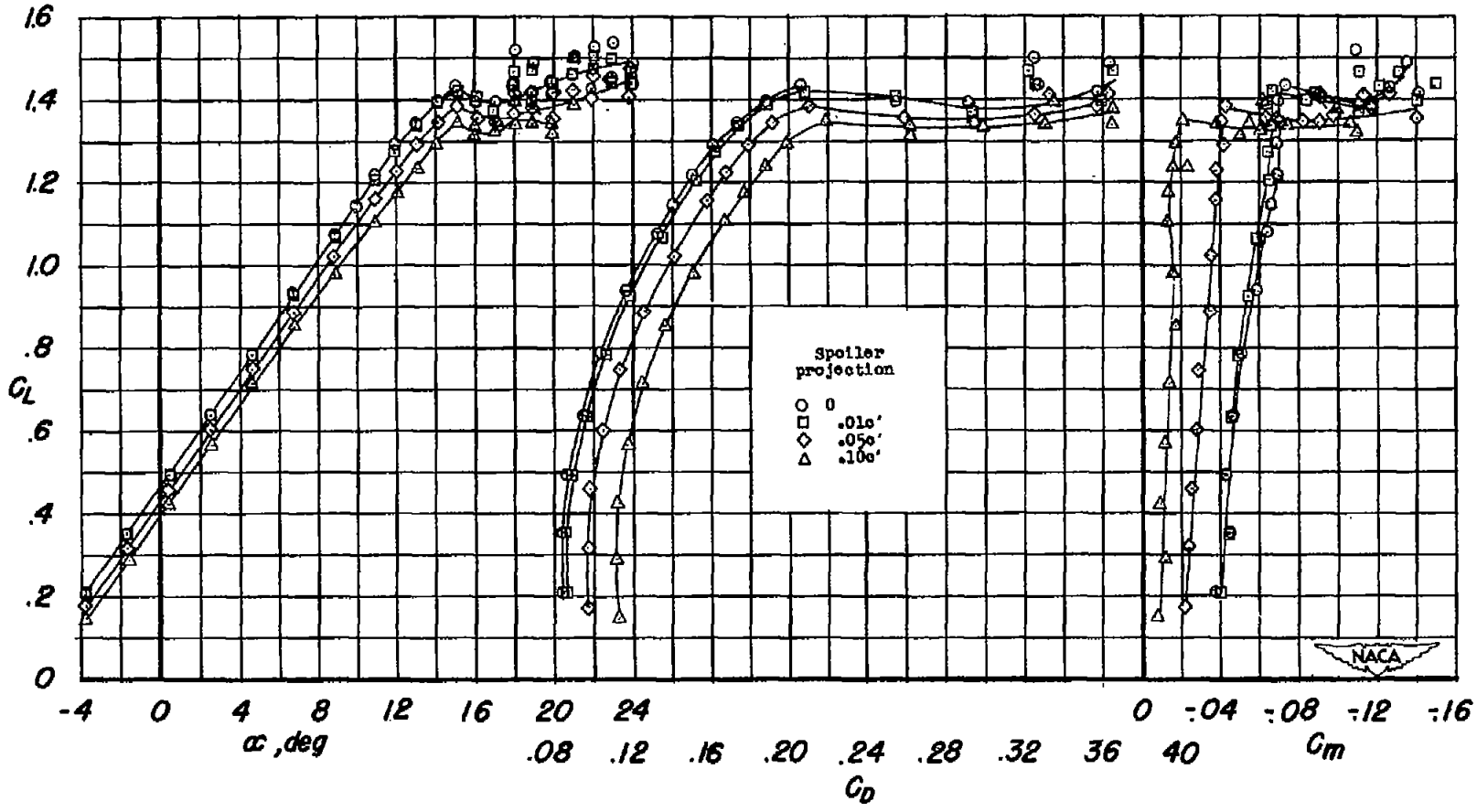

(a) Lift, drag, and pitching moment.

Figure 26.- Effects of half-span spoilers at 0.65c' on the aerodynamic characteristics of a 37° sweptback wing with leading-edge slat and semispan split flap. $R = 6.8 \times 10^6$.

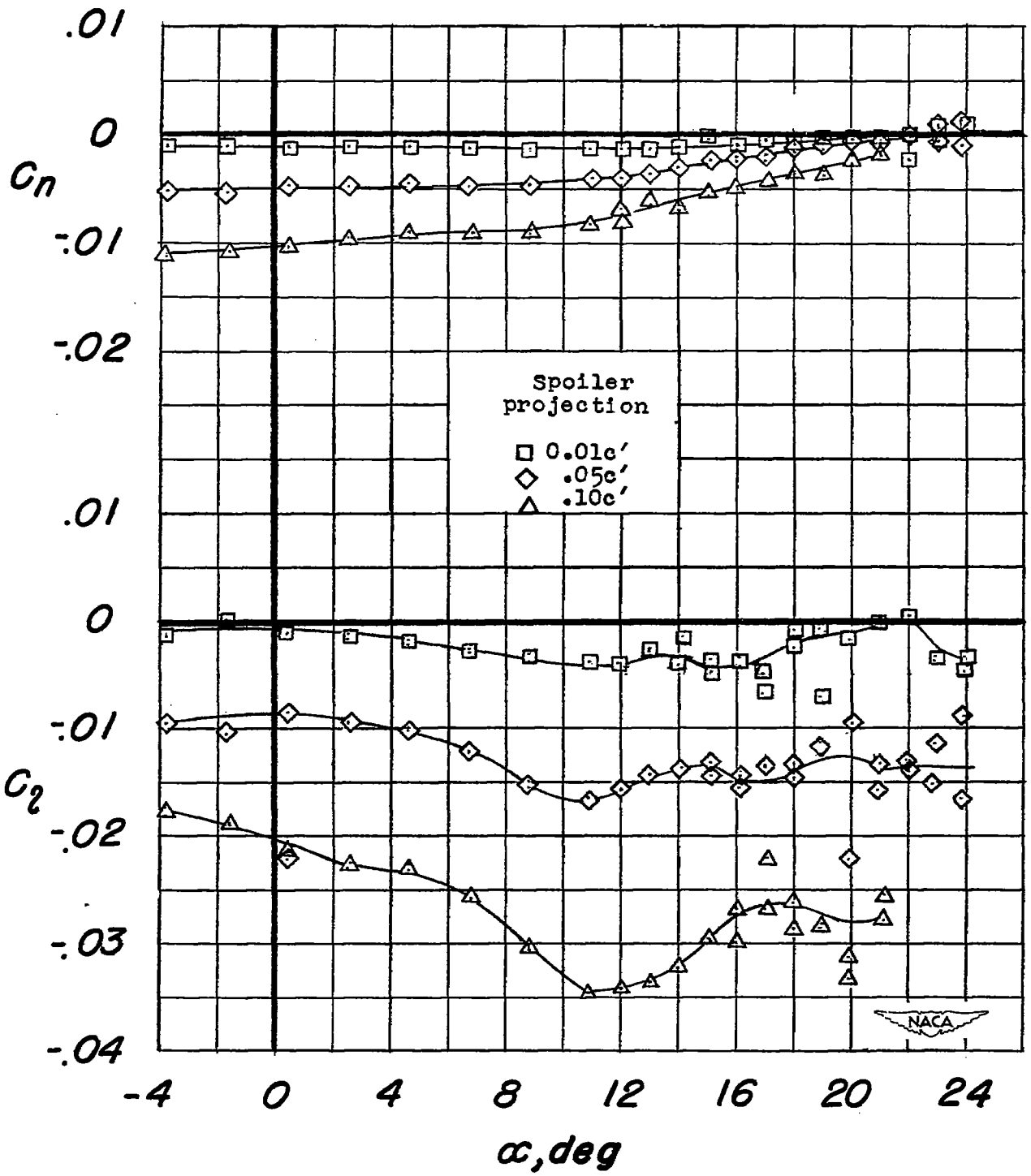

(b) Rolling moment and yawing moment.

Figure 26.- Concluded.

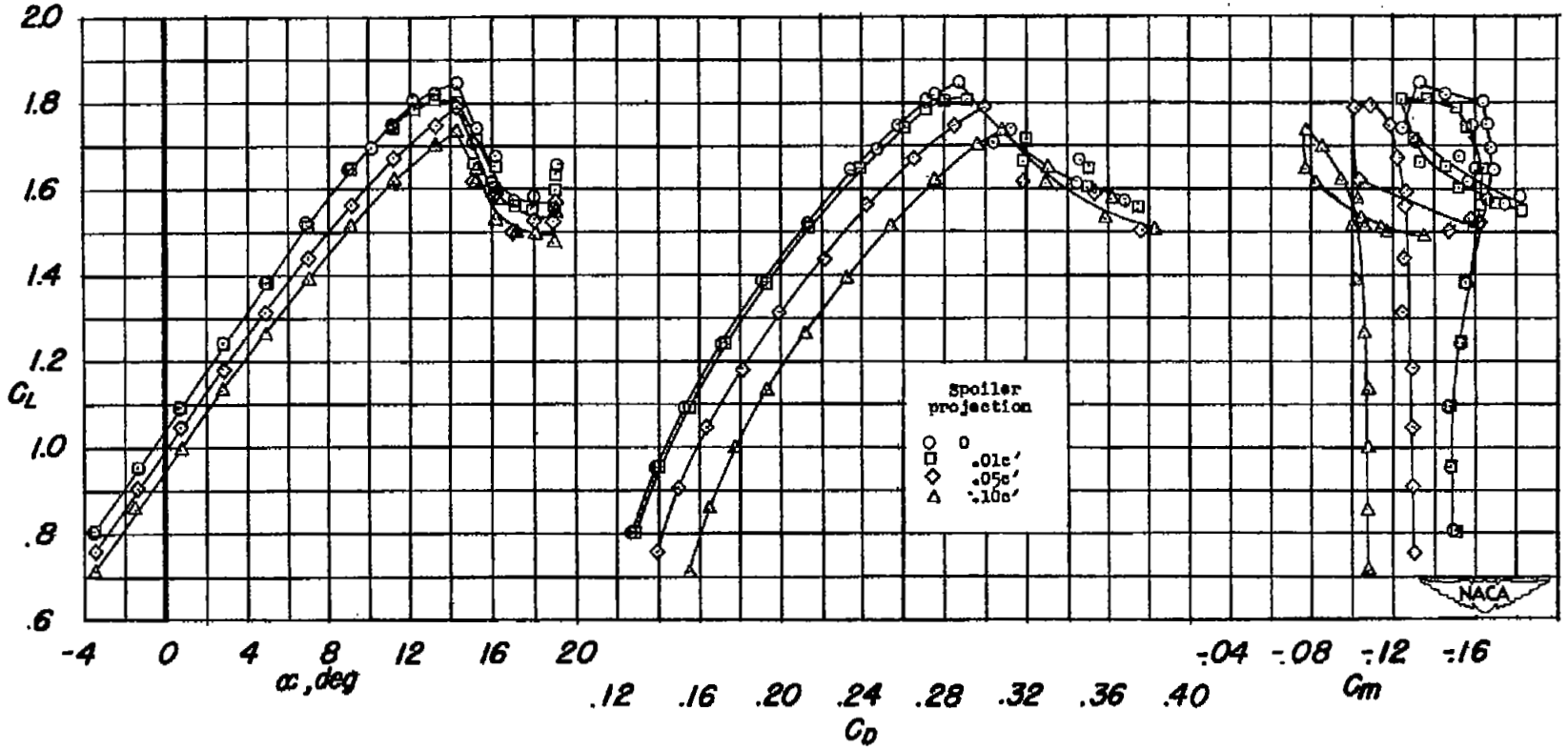

(a) Lift, drag, and pitching moment.

Figure 27.- Effects of half-span spoilers at 0.65c' on the aerodynamic characteristics of a 37° sweptback wing with leading-edge slat and semispan double slotted flap. $R = 6.8 \times 10^6$.

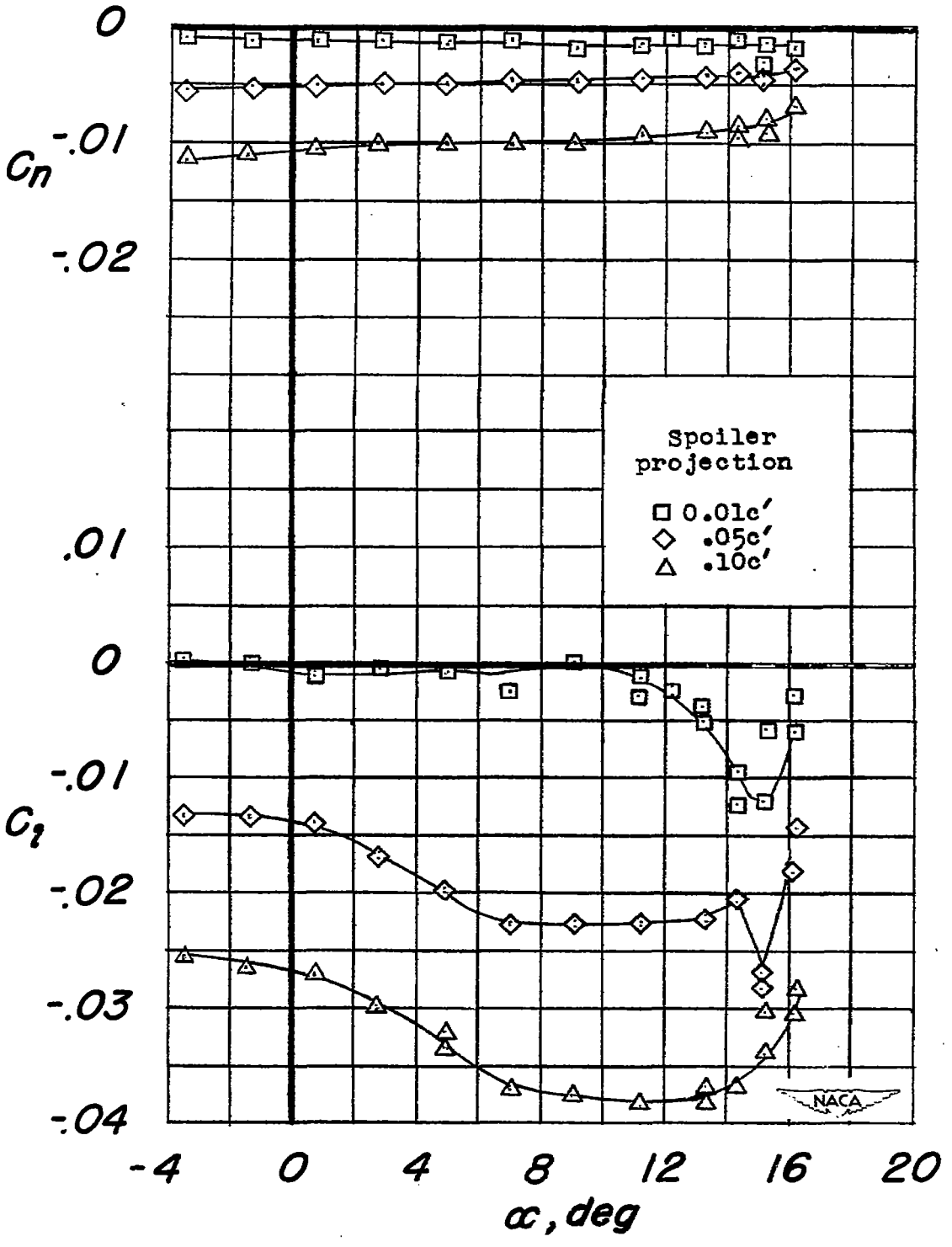

(b) Rolling moment and yawing moment.

Figure 27.- Concluded.

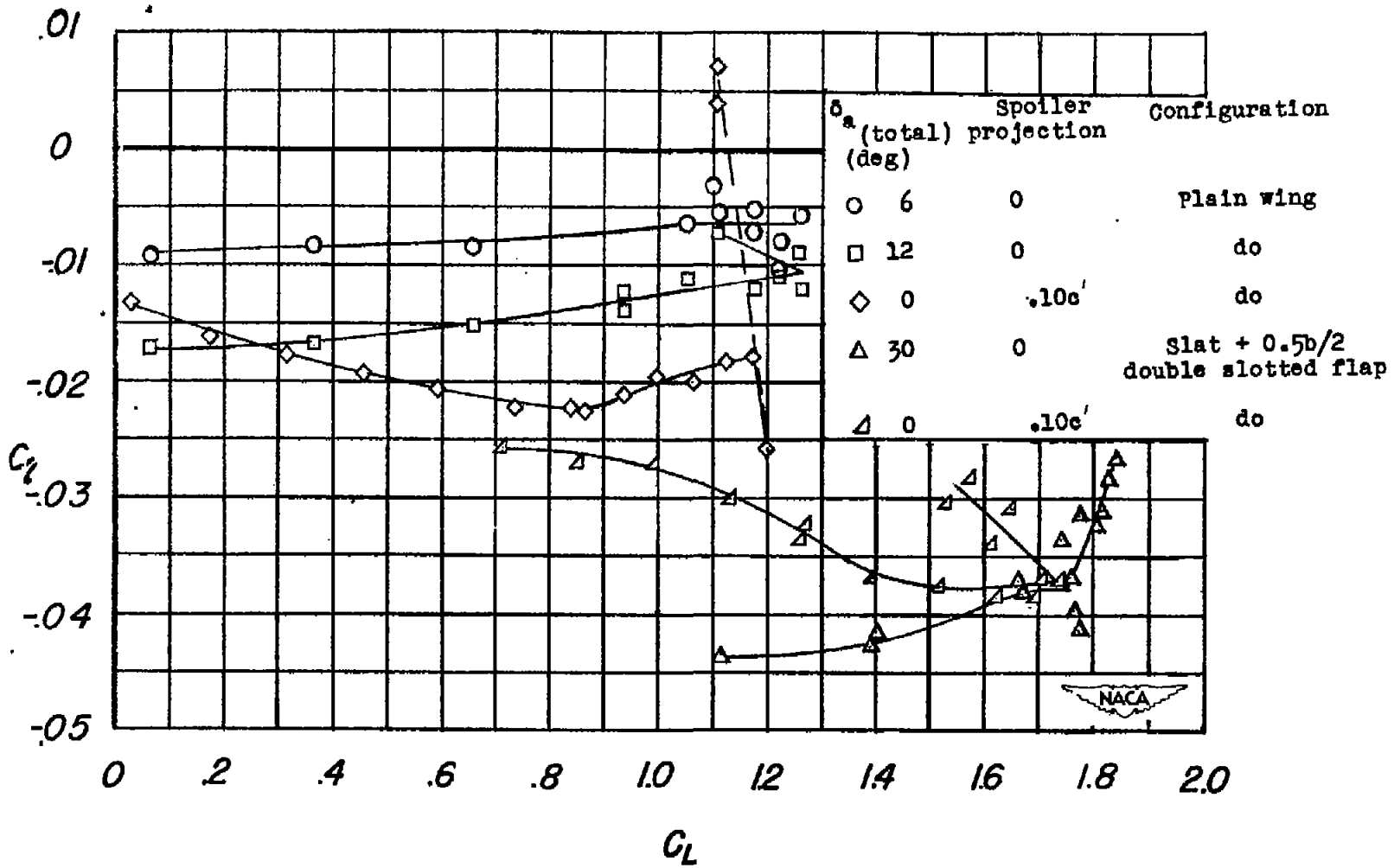

Figure 28.- Comparison of rolling moments of aileron and plain spoiler at 0.65c' on a 37° sweptback wing. $R = 6.8 \times 10^6$.